Demographic causes of the pesticide crash in the peregrine falcon

Marc Kéry[1,3], René-Jean Monneret[2], Jaume A. Badia-Boher[1], & Michael Schaub[1]

[1] Population Biology Research Unit, Swiss Ornithological Institute, Seerose 1, 6204 Sempach, Switzerland

[2] Moulin du Haut, 39140 Arlay, France

[3] contact & corresponding author: marc.kery@vogelwarte.ch

Open Research

Data and R and JAGS code used in this publication will be posted on Zenodo upon acceptance. They are currently here (see this LINK).

Key-words: autoregressive smoothing; cyclodiene; DDT; demography; Dieldrin, ecotoxicology, integrated population model (IPM); pesticide crash; random effects, time-series

Abstract

Population crashes in many avian predators during the 1950–70s, caused by organochlorine pesticides, belong to the most spectacular cases in the history of conservation and ecotoxicology. Negative effects of DDT on eggshell thickness, leading to egg breakage and declining productivity, are well-documented. In addition, cyclodiene pesticides such as Dieldrin were strongly suspected to contribute to crashes by increasing mortality, but the hypothesis of a contribution of survival to the crash could never be tested directly owing to a lack of early enough data and suitable analyses. We studied the demography of a large population of the peregrine falcon (*Falco peregrinus*) in the Jura mountains over 60 years (1964–2023), from crash to recovery. We combined in an integrated population model ring-recovery, productivity and population count data, tested for a reduction in survival during crash years and used retrospective analysis to compare the relative importance of survival and productivity for population dynamics. Incidentally, we discovered that for data with unequal sample sizes over time, only an autoregressive time-series formulation properly captured annual trajectories of demographic parameters, while traditional models with unstructured temporal random effects, assuming stationarity, did not. The population crash continued until the early 1970s, and subsequent recovery was not complete until the early 2000s. Productivity was greatly reduced during the crash and increased afterwards. Between 1964 and 1978, adult survival was strongly reduced, recovering from 0.62 (0.46–0.75) to 0.85 (0.77–0.91), while juvenile survival showed a long-term decline. The variance of the population growth rate was primarily explained by adult survival (67%), followed by productivity and juvenile survival (16% each). Hence, our study reveals an overwhelming effect of adult survival rather than productivity in the pesticide crash and recovery in this peregrine population. This is arguably the first time that the hypothesis, that survival was the major cause of the pesticide crash, was tested and corroborated. The success of our detective story illustrates well the key role of intensive long-term monitoring schemes: in combination with modern analytics, they can generate critical demographic knowledge with wide conservation implications and thus serve as invaluable environmental early-warning systems.

Introduction

Understanding the dynamics of natural populations lies at the heart of ecology. Sometimes, extreme events lead to extreme dynamics, such as population crashes or even extinction. Two of the most highly publicized cases of such crashes during the last 100 years involved vultures in South Asia during the 1990s (Oaks *et al.* 2004) and several raptor species feeding on birds and fish in most parts of the world in the 1950s–1970s (Hickey & Anderson 1968, Hickey 1969). Perhaps owing to the extraordinary magnitude of the declines, it soon became apparent that only a small number of causes could be involved. And indeed, the main mechanisms underlying both crashes were identified within about a decade.

In both, chemical substances widely used in agriculture proved to be the culprits. In the former, the use of Diclofenac in cattle breeding caused renal failure in vultures who fed on carcasses contaminated by Diclofenac and led to catastrophic mortality (Oaks *et al.* 2004). In the latter, organochlorine pesticides such as DDT were shown to be responsible, leading to reductions in eggshell thickness, increases of egg breakage and declining productivity. This resulted in strong population declines in all affected species (Newton 1979, 1998, Ratcliffe 1993), and produced what has since been dubbed the 'pesticide crash'. For instance, in the entire eastern half of the Unites States the iconic peregrine falcon (*Falco peregrinus*) became extinct during the 1960s, while this huge area had originally hosted several hundred pairs (Hickey 1969). Likewise, thousands of pairs in Fennoscandia were diminished to barely a few dozen right after the crash (Cade *et al.* 1988).

In lab experiments and observational studies, DDT was shown to lead to egg-shell thinning in many bird species (Ratcliffe 1967, 1970, Hickey & Anderson 1968), causing egg breakage and greatly reduced productivity, and in addition may also be directly toxic (Wurster *et al.* 1965, Van Velzen *et al.* 1972). Indeed, reduced productivity was a hallmark of the crash in all species affected (Cade *et al.* 1988). However, especially in Europe, Newton (1979, 1998), Ratcliffe (1993) and Sibly et al. (2000) pointed out that crashes were too drastic to be caused by decreased productivity alone and suggested that reduced survival was a major factor in the crash. In Europe, cyclodiene organochlorine pesticides such as Dieldrin were widely used as seed-dressings just prior to the crash and were known in several cases to cause catastrophic mortality in birds, occurring at lethal levels in the bodies of birds found dead (Ratcliffe 1993, Newton 1979, 1998). But however well-founded the hypothesis of reduced survival as a driver of the crash was, it could never be tested directly. This was mostly due to the lack of demographic data that reach back far enough in time and perhaps also for a lack of

adequate modeling, as we will see. Hence, the relative roles of survival and productivity in the pesticide crash have remained unassessed until now (Greenwood 2021, Oli *et al.* 2023).

Here, we fit a matrix population model to a combination of population counts and productivity data from two adjacent, long-term peregrine population studies in the Jura mountains of Switzerland and France over 60 years (1964–2023), starting in the years even before the nadir of the crash. We jointly analyse these data in an integrated population model (IPM; Besbeas *et al.* 2002; Schaub & Kéry 2022) alongside Swiss ring-recovery data. The early start of these studies with respect to the darkest years of the crash and the availability of ringing data from these years provide a unique opportunity to investigate temporal trends in survival and recovery in a population severely hit by the crash. In particular, it allows us to test whether survival was abnormally low during the crash years, as predicted by Newton (1979, 1998) and Ratcliffe (1993).

Crucially, to infer trajectories of survival and productivity over time we did not adopt the usual unstructured temporal random effects that are so widely used for 'batches' of similar parameters (Gelman 2005). These assume a stationary process over time and the resulting *'global smoothing'* of annual estimates is likely to mask important time trends when stationarity does not hold and when sample sizes vary over time, as they naturally will in a population affected by catastrophic dynamics. To overcome these problems, time-series modeling for these parameters is required (Johnson & Hoeting 2003; Link & Barker 2010: chapter 10; Hefley *et al.* 2017). The resulting *'local smoothing'* avoids problems due to unequal amounts of information over time produced by varying sample sizes. To highlight the risks of uncritical random-effects modeling assuming stationarity, we compare time-series inferences with those under the traditional model with unstructured random effects.

Our main goal was to investigate the relative roles of survival *vs* productivity and therefore, by implication, primarily of cyclodiene pesticides such as Dieldrin *vs* DDT in the pesticide crash in a large population of the peregrine falcon. A reduction not only of productivity but also of survival during the crash years would corroborate the hypothesis that survival and cyclodienes had an important role in the pesticide crash, as predicted by Ratcliffe (1993) and Newton (1998). We take advantage of time-series modeling of demographic parameters, and of two extraordinarily long time-series of population data collected by dedicated citizen scientists. This and the combination in an IPM of all data from both studies maximizes our power to reveal temporal patterns in the demographic parameters over the full 60 years.

Study species, study area, and field methods

Study species

The peregrine falcon is a medium-sized raptor with a worldwide distribution (Cade 1982). In Western Europe, peregrines nest mostly on cliffs and sometimes on buildings and often use the same nesting site for decades (Ratcliffe 1993). In our study area, peregrines lay 3–4 eggs in March that hatch after about 30 days of incubation. Nestlings fledge in late May and early June around 42 days of age (Monneret 2017). The peregrine is arguably the most iconic of the victims of the pesticide crashes in many parts of the world during the 1950–70s, when it became regionally extinct or very rare in vast parts of North America and Europe (Hickey 1969; Cade *et al.* 1988; Sielicki & Mizera 2009). Dramatic reductions in its productivity during the crash years are very well-documented (Newton *et al.* 1989, Ratcliffe 1993). In contrast, an important role of survival in the crash has been strongly hypothesized (Newton *et al.* 1989, Ratcliffe 1993), but could never be shown so far.

Study area

Our study area comprised most parts of the Jura mountains (46°45'N, 5°54'E) in France and Switzerland and adjacent areas in southwest Switzerland (Appendix S1). The Jura is a limestone range with elevations up to 1718 m and extends over more than 300 km from southwest to northeast, being about 100 km at its widest. It is sparsely populated by humans and forest cover amounts to almost 50%. Suitable limestone cliffs for nesting abound and host a large and fairly dense peregrine population that currently numbers more than 250 breeding pairs in about 420 known territories (Kéry *et al.* 2022).

Field methods

Peregrines in the Jura mountains have been the subject of two long-term population studies since the early 1960s. Here, we combined in a single analysis their demographic data over 60 years (1964–2023). The study on the Swiss side comprised about 5,000 km^2 in the southwestern tip of Switzerland, most of it in the Jura, but also including some adjacent regions on the Plateau and along the northern fringe of the Alps (Appendix S1). This study was led by the late Gabriel Banderet until 2016, and afterwards by members of the Swiss Ornithological Institute (Jérémy Savioz, Jérémy Gremion). The study on the French side comprised the three departments Ain, Jura and Doubs, for a total of about 11,460 km^2, and has been led by René-Jean Monneret and the Groupe Pèlerin Jura (Monneret *et al.* 2019).

Field methods were similar in both studies. Each spring, the teams tried to visit as many previously known territories as possible and to check a large number of other, potential nesting cliffs in search of new pairs, typically conducting multiple visits per site each spring. The number of pairs counted per year was taken as the usual measure of population size. During the nestling stage, cliffs with pairs were visited and brood size was assessed by counting young during the mid to late nestling stage (i.e., at 21 days or older) with 20–60x telescopes, sometimes during ringing (see below), and occasionally also after fledging at sites where it was impossible to view the eyries. In the French study, unsuccessful broods were not consistently recorded. Hence, we ignored the French broods with recorded size of zero and treated French brood size as zero-truncated in our analysis. In the Swiss study, about 2,200 chicks were ringed during 1964 and 2014 (Appendix S2). This included the efforts of another team led by Michel Juillard in the northern parts of the Swiss Jura during the 1980s and 1990s. Some 160 (7%) individuals ringed as nestlings were later recovered dead, providing data that directly inform our models about survival probability.

Population modeling

For inference about peregrine demography, we used an integrated population model (Besbeas *et al.* 2002; Schaub & Kéry 2022). That is, we formed the joint likelihood for all data sets which, under the usual assumption of independence, is given by the product of a state-space likelihood for the population counts, a hurdle Poisson regression for productivity, and a ring-recovery model for the dead-recovery data. Note that our analysis is an improved version, for a much longer time-series of data, of that in Schaub & Kéry (2022: Chapter 12).

We structured our population model according to a pre-breeding "census", where the population is observed in March, and where four age/stage classes are distinguished: first-year birds that do not breed, second-year birds that do not yet breed, second-year birds that do breed, and birds aged three years and older that are all assumed to breed at rate θ, which denotes the productivity rate, i.e., the number of young produced per breeding pair (Appendix S3). Population dynamics is represented by a first-order Markov process where the number of individuals in each stage class at time t+1 is a function of their number at time t, and of a transition matrix containing demographic parameters for survival and productivity. We assumed two age classes for survival: juvenile or first-year survival s_1, i.e., from fledging in May of year t to March of year t+1, and adult survival (s_2) from March in year t to March in year t+1. We further assumed that only a fraction α of second-year birds reproduced.

For each country, our stage-classified population model is thus given by the following four equations, in which Poisson and binomial distributions are used to accommodate demographic stochasticity:

$$N_{1,t+1} \sim \text{Poisson}(0.5 \times \theta_t \times s_{1,t} \times (N_{3,t} + N_{4,t}))$$

$$N_{2,t+1} \sim \text{Binomial}(s_{2,t} \times (1-\alpha), N_{1,t})$$

$$N_{3,t+1} \sim \text{Binomial}(s_{2,t} \times \alpha, N_{1,t})$$

$$N_{4,t+1} \sim \text{Binomial}(s_{2,t}, N_{2,t} + N_{3,t} + N_{4,t})$$

The number of breeders (i.e., $N_{3,t} + N_{4,t}$) in year *t* was linked to the observed counts y_t with a Poisson log-normal distribution, where Gaussian noise terms account for extra-Poisson temporal variability in the counts, i.e., as $y_t \sim \text{Poisson}((N_{3,t} + N_{4,t}) \times \exp(\varepsilon_t))$, with $\varepsilon_t \sim \text{Normal}(0, \sigma^2)$. We allowed σ^2 to vary by study area to account for possibly different precision of the counts.

We decomposed productivity rate θ into two parts, brood success (ψ) and conditional brood size (ρ). The former is the probability that a pair successfully raises a brood, i.e., that it produces at least one young, while the latter is the mean brood size given that a brood is raised, i.e., mean size of broods excluding zeroes. The result is a Poisson hurdle model (Dorazio *et al.* 2013), which can be represented hierarchically as a combination of a Bernoulli random variable for brood success and a truncated Poisson random variable for conditional brood size, and where mean annual productivity is given by $\theta_t = \frac{\psi_t}{1-\exp(\rho_t)}\rho_t$.

We chose the hurdle formulation for biological and practical reasons. First, different processes may govern whether a brood is raised at all, and the number of young produced if a brood is raised. This will often lead to brood size data that are zero-inflated relative to a Poisson. The hurdle model represents two such processes and therefore naturally accommodates zero-inflated brood size. Second, our French brood size data were zero-truncated, and a hurdle model allowed their seamless integration in the analysis under the assumption that brood success was identical in both study areas.

We formulated the ring-recovery part of the IPM for an m-array summary of the data, where cell probabilities are functions of juvenile and adult survival and of a recovery probability that is assumed to be identical for both ages (Brownie *et al.* 1985). We expressed recovery probability as a logistic function of the year to allow for a possible decline, as has been widely observed (Robinson *et al.* 2009).

In summary, we described peregrine population dynamics by five demographic parameters: juvenile and adult survival (s_1 and s_2), recruitment probability of second-year birds (α), brood success probability (ψ) and conditional brood size (ρ). We assumed α to be constant over time, since experimentation with time variation in this parameter yielded extremely imprecise estimates, suggesting that our data did not permit estimation of such a pattern. At the same time, we noted a remarkable robustness of all other parameter estimates to different specifications of recruitment probability, α. Hence, we think that our results are not affected by the somewhat artificial modeling choice of a constant α.

All other demographic parameters were allowed to vary by year. As a result, our models contain 59 survival and 60 productivity parameters. The most widespread approach to estimation of such 'batches' of parameters is to treat them as exchangeable, or as temporally unstructured random effects (Gelman 2005). After applying a suitable link function, they are treated as draws from a normal distribution with a shared mean and variance, and these hyperparameters are estimated from the data. One consequence in the context of a time-series of parameters is that each year's estimate borrows strength from the ensemble of all years. This leads to shrinkage as a sort of global smoothing, where each year's estimate is pulled towards the constant shared mean of the time-series (Burnham & White 2002). The degree of shrinkage is determined in part by the amount of information about each year's parameters: parameters for which there is little information in the data are pulled in more towards the shared mean. Shrinkage in random-effects estimation can be beneficial in reducing estimation error (Kéry & Royle, 2021: Section 3.3).

However, the adoption of unstructured temporal random effects critically requires the exchangeability assumption for the entire time-series of parameters, also called stationarity. Hence, the validity of such traditional random-effects estimates rests on the assumption that they all share a common mean and variance. For long parameter time-series and for large changes in the population dynamics of a species, this assumption may easily be violated. In this case, we need alternative formulations of temporal random effects, which allow for a smoothly varying mean over time. These lead to local rather than global smoothing of the series, where the amount of shrinkage for the estimate in year *t* is governed primarily by the years surrounding *t*, and not by all years in the series. In other words, we need a proper time-series formulation for time-varying parameters (Johnson & Hoeting 2003, Link & Barker 2010, Hefley *et al.* 2017). We used a random-walk formulation of temporal autocorrelation in the demographic parameters (Link & Barker 2010: chapter 10), where the value of a time-

series of parameter ϕ, at a suitable link scale g, is expressed as $g(\phi_{t+1}) \sim \text{Normal}(g(\phi_t), \sigma^2_\phi)$ and the initial parameter ϕ_1 of the series is estimated by placing a prior on it. Below, we compare the inferences under the random-walk model with those under a traditional model with unstructured temporal random effects, which assumes stationarity of parameter time-series. BUGS code for the random-walk model is given in Appendix S4.

Based on the parameter estimates from the random-walk model for Swiss and French data combined, we then conducted a retrospective analysis (transient life-table response experiment, or tLTRE; Koons *et al.* 2016, 2017). We decomposed the temporal variance of the observed annual population growth rate into contributions from time-varying demographic rates and population structure. We thus assessed the degree to which temporal variability of demographic rates and population structure, and their temporal covariation, contributed to the variation in the observed population growth rate during our study period.

We conducted a posterior predictive check to test the goodness of fit (GoF) of the model with random walk, using the Freeman-Tukey statistic as a discrepancy measure (Kéry & Royle, 2016: Chapter 2). This suggested adequate fit for the Swiss data, but moderate lack of fit of the French data, especially for the French fecundity data (Appendix S5). However, this lack of fit went into the opposite direction of what is usually seen for a model that fails a GoF test: data simulated under the model were more variable than the actual data. That is, we found a case of underdispersion, which is perhaps not surprising for brood size. In addition, refitting the model without the French productivity data (unpub. analysis) led to no relevant change in the posteriors of our key estimands, juvenile and adult survival. For these reasons, we assumed that the lack of fit of the model for the French data was innocuous.

We used Bayesian inference and fitted the IPMs using MCMC techniques in program JAGS (Plummer 2003), run from R (R Core Team 2019) via the 'jagsUI' package (Kellner 2024). We ran four chains to convergence, as judged by visual inspection of trace plots and by values of the Brooks-Gelman-Rubin statistic Rhat < 1.1 (Kéry & Royle, 2021: Chapter 2).

Results

Evolution of population size during the 60-year study period

Peregrine population levels were different in the Swiss and French study areas, but the shape of the population trajectory was similar: the minimum population size was reached around 1970 and full recovery 30 years later, by the early 2000s (Fig. 1). In the Swiss subpopulation,

only six pairs were left in 1964 and further decline led to local extinction in several years between 1971 and 1976. This was followed by recovery to about 50 pairs during 2000–2011, with another decline to around 40 pairs towards the end of the study period. In the much larger French subpopulation, numbers declined from 58 pairs in 1964 to a minimum of ~20 in 1969–1972. and then recovered to about 200 pairs during 2002–2023.

Comparison of two models with random time effects for the Swiss data

We first explored two IPM formulations for the more complete Swiss data. We fitted one traditional IPM with unstructured random time effects for all vital rates around a constant mean, i.a., assuming stationarity, and another IPM with a random walk for the vital rates (Fig. 2). The estimated logistic regression of recovery probability was very similar, showing a decline over time (Appendix S6), but the temporal patterns inferred for all four demographic parameters were very different. The IPM with unstructured temporal random effects suggested mere fluctuations without any long-term trend during the entire 60 years. In sharp contrast, the random-walk model suggested recovery of adult survival, brood success, and conditional brood size over the initial 10–30 years, and a long-term decline in juvenile survival over the entire study period. So, which model should we now use for inference about peregrine demography during the crash?

Different smoothing behaviour elucidated by a simple case study with Swiss productivity

To better understand the behaviour of the two models with global and local smoothing, we first investigated Swiss productivity alone, since here we can compare estimates under both models with the observed data. It is very well known that peregrine productivity was strongly depressed during the crash (Hickey 1969, Cade *et al.* 1988, Ratcliffe 1993), and this provides a strong expectation to gauge the inferences from an adequate model. We fitted two IPMs to the Swiss data that had either unstructured random or random-walk random effects of time in juvenile and adult survival and productivity and did not decompose the latter.

Figure 3 shows the observed time-series of mean productivity, with symbol size proportional to sample size, i.e., the number of broods. Information on brood size before 1980 is scarce, but by this time productivity had already fully recovered. Due to the imbalance in the data, the estimates under the traditional random-effects IPM with unstructured random time effects (red polygon) are largely informed by the post-crash years. Therefore, the estimates during the crash years are strongly shrunk towards the post-crash mean and this completely masks the strong reduction of productivity during the crash. In

contrast, the IPM-based estimate with a random-walk (blue polygon in Fig. 3) closely reflects the observed time-series of the demographic parameter.

Analogous behavior is apparent when fitting two simple regression models to the productivity data alone, one with a constant mean and the other with a spline of year, i.e., another local smoothing technique. The model with constant mean (red line in Fig. 3) completely misses the extraordinariness of the crash years, while the spline model (blue line in Fig. 3) correctly identifies this crucial demographic pattern. Indeed, the estimates of the latter are very similar to those from the random-walk IPM. Therefore, we assumed that only the random-walk model adequately captured the temporal patterns in the parameters driving peregrine falcon demography. As a result, we used the random-walk model for inferences about demography for the combined data from the Swiss and the French studies.

Inferences about demographic rates under the random-walk model

From estimates for both studies combined, juvenile survival declined from a maximum of 0.62 (95% CRI 0.37–0.87) in 1974 to a minimum of 0.43 (0.25–0.59) in 2015 (Fig. 4a). During the crash years, adult survival was strongly depressed, and during the initial 14 years, i.e., from 1964 to 1978, it greatly increased from 0.62 (0.49–0.75) to 0.85 (0.77–0.91) and fluctuated afterwards (Fig. 4b). Brood success probability increased from 0.53 (0.33–0.68) in 1964 to 0.64 (0.54–0.77) over the initial 13 years and likewise fluctuated afterwards (Fig. 4c). Conditional brood size increased from 1.31 (1.05–1.59) in 1964 to 2.39 (2.23–2.57) in 1997 and declined somewhat later (Fig. 4d). Thus, three of four demographic parameters showed a strong increase during the 1960s and 1970s or even later. Comparing the estimated adult survival at its maximum in 1978 with that in 1964 yields a probability of >0.999 for a reduction of adult survival during the pesticide crash (Fig. 5). See Appendix S7 for posterior summaries of all parameters under the random-walk model.

To check for the robustness of the key result on the drop of adult survival during the crash, we conducted a prior sensitivity analysis where we re-fitted the model with four different informative priors for the two initial survival probabilities in the 1964–1965 interval (Appendix S8). This revealed moderate prior sensitivity for juvenile survival during the initial 10–20 years, but almost no sensitivity to prior choice of adult survival or juvenile survival later on. Thus, in spite of the small sample size of the ring-recovery data during the crash years, our findings about adult survival appear to be remarkably robust.

Predictions of population size under our IPM agreed well with the observed trajectory of population sizes in both study areas (Appendix S9). Estimated state structure distributions

for both study areas separately are shown in Appendices S10 and S11. They show how the estimated proportion of nonbreeders, or floaters, declined in Switzerland from about 0.5 during the mid-1970s to about 0.3 during the recent decade, but remained approximately constant near 0.4 in France.

Relative effects on population dynamics of vital rates and population structure

Retrospective analysis by tLTRE revealed that adult survival explained a full two third (67%) of the observed variance in the population growth rate, while juvenile survival and the two productivity components combined explained 16% each. The contribution of changes in the population stage structure to population growth was negligible (Fig. 6).

Discussion

Demographic process and patterns of the pesticide crash

Population crashes in many raptors during the 1950s–1970s, caused by organochlorine pesticides, are among the most dramatic declines known of any vertebrate population. However, the demographic mechanisms underlying this 'pesticide crash' were only implied (Ratcliffe 1993, Newton 1998, Sibly *et al.* 2000), but until now have not been tested directly. Specifically, the relative roles of DDT, leading primarily to reproductive failure, and of cyclodienes such as Dieldrin, leading to increased mortality, have never been assessed in any wild population, due to the lack of long-enough ringing data and adequate analytical methodology. All previously published survival analyses on affected species, such as Mearns & Newton (1984), Smith *et al.* (2015) or Robinson & Wilson (2021), used data from the 1970s or later, missing most or all of the crash years in their study region. Sibly *et al.* (2000) is a theoretical study showing how a reduction in survival causes decreased population growth in the sparrowhawk *Accipiter nisus*.

Here, in a 60-year study of a large population of the peregrine, one of the species most affected by the crash, we found greatly reduced adult survival during the crash years and a dominant influence of adult survival on the observed population dynamics. This is the first time that the role of survival in the pesticide crash could be directly demonstrated for any species in the wild. Our study thus confirms the prediction that reduced survival had a crucial role in the crash (Newton *et al.* 1989, Ratcliffe 1993, Newton 1998, Sibly *et al.* 2000, Greenwood 2021, Oli *et al.* 2023).

In the Jura peregrine population, recovery slowed over time as one expects for any population regulated by density-dependence and was complete after about 30 years. From our demographic estimates (Appendix S7), generation time can be estimated at 5.5 years (Caswell 2001). Thus, it took about five generations for the population to reach a new more or less stable level, showing how exceptional of a catastrophe the pesticide crash was.

Not all demographic rates exhibited the same temporal trajectory: adult survival was essentially back to normal by the late 1970s, while conditional brood size reached a plateau only by the early 2000s. This is probably due to different persistence rates of the pesticides involved (Ian Newton, pers. comm.). In soils, the half-life of DDE (the chemical derivative of DDT) is 12–57 years and that of dieldrin only 2.5 years, while in live pigeons the corresponding values are 240 days and 47 days, respectively (Newton 1998: p. 418, 420). Incidentally, this pattern suggests a dominant effect of DDT on productivity rather than survival in the Jura peregrine population (Pierre Bize, pers. comm).

Juvenile survival was apparently not affected by the pesticide crash but rather declined over the entire study period. Density-dependence may be causing this effect on what presumably are the weakest individuals in the population. This may have been exacerbated during the most recent years by the recovery in the Jura of the main predator of the peregrine, the Eurasian eagle owl (own unpublished data). Its predation may again disproportionally affect the most naïve individuals in the population, especially after fledging. In addition, organochlorine pesticides bioaccumulate with age and it may take some years before they reach high, toxic levels. Thus, negative effects of pesticides may be detected primarily on adult rather than juvenile survival.

The relative roles of DDT, causing reproductive failure for the most part, and of cyclodienes, causing survival failure, in North America as opposed to Europe have been debated (Newton *et al.* 1989, Ratcliffe 1993, Greenwood 2021). In North America, temporal patterns and the relative magnitude of the use of the two types of organochlorine pesticides and of the pesticide crash suggested a dominant role of DDT rather than of cyclodienes. In contrast, in Europe, analogous evidence pointed to a major role of cyclodienes. This latter hypothesis thus finds corroboration by our study.

The importance of the "right" random effects modeling in demographic studies

One key to our success in unraveling the role of adult survival in the pesticide crash and subsequent recovery was the use of a random-walk that accommodates nonstationarity in the series of annual parameters and accounts for temporal autocorrelation. Traditional

unstructured temporal random effects for the demographic parameters smooth a time-series globally. As a consequence, years with large samples will dominate the estimates. If sample sizes vary greatly over time and the modelled process is not stationary, very wrong inferences about a time-series of parameters may result. This was evident for Swiss productivity, where traditional random-effects modeling completely missed the substantial reduction of this demographic rate during the crash. Presumably, the same also happened with the estimates of the other demographic rates in this model. In contrast, the random-walk model with its local series smoothing correctly identified strong reductions in three of the four modelled demographic rates during the crash years.

Our results thus highlight the importance of the stationarity assumption in the random-effects modeling of time-series of parameters. Arguably, this assumption becomes less tenable with longer time-series. Given that more and more demographic analyses are conducted for long-term population studies, we believe that this is an important methodological take-home message. In addition, local smoothing allows detecting time variation with considerably lower and uneven sample sizes. Many population studies may be constrained by limited sample sizes, especially when using "expensive" methods such as capture-recapture, and when dealing with rare or low-density species, where sample sizes will inherently be low. In these situations, analysts should probably consider random effects with local rather than global smoothing.

Importance of long-term population studies … and of the citizen-scientists conducting them

We were privileged to have access to data from two very long-term population studies that started in 1964 and thus well before the lowest point of the crash in our study area. The availability of such very long time-series of population data was decisive for our ability to uncover the role of adult survival in the crash and the recovery. In particular, the very early ringing data were instrumental for our ability to estimate survival during the crash years.

Our study emphasizes the huge value of long-term ecological research. Importantly, long-term population studies have frequently been conducted by amateurs. Often unnoticed in the professional literature, these people render a tremendous service to science. There is a sense in which these original citizen scientists are the unsung heroes of population ecology; may they be warmly thanked.

The data produced by such long-term population studies enable much deeper mechanistic insights into observed population trends. Thus, long-term population studies, especially of environmentally sensitive species such as the peregrine (Castagna *et al.* 2024), serve not only

as early-warning systems when "something is wrong" (Oli *et al.* 2023). But, when paired with sound demographic modeling, they can also identify the causes behind the change in terms of the underlying demographic mechanisms. This is not only a big advantage in terms of scientific understanding, but may also be a key for attempts to "right the wrong".

Acknowledgements: All the people who conducted the field work and most of all the Gabriel Banderet and René Ruffinoni, as well as all the other members of the *Groupe Pèlerin Jura* (GPJ), Michel Juillard, Simon Lovis, Michel Rebetez, Jean-Marie Gisiger and their colleagues on both sides of the border in the Jura mountains. Through their dedication and tenacity, they made this study possible in the first place. We thank Ian Newton and Pierre Bize for many valuable comments, and Liv Fritsche for the map in Appendix S1.

Conflicts of interest Statement

The authors declare no conflicts of interest.

References

Besbeas, P., Freeman, S.N., Morgan, B.J.T., Catchpole, E.A. 2002. Integrating mark-recapture-recovery and census data to estimate animal abundance and demographic parameters. *Biometrics*, 58, 540–547.

Brownie, C., Anderson, D.R., Burnham, K.P., Robson, D.S. 1985. *Statistical Inference from Band Recovery Data - a Handbook*. U.S. Fish and Wildlife Service, vol. 156. Duxbury Press, Washington D.C.

Burnham, K.P., White, G.C. 2002. Evaluation of some random effects methodology applicable to bird ringing data. *Journal of Applied Statistics*, 29, 245–264.

Cade, T.J. 1982. *Falcons of the World*. Cornell University Press, Ithaca, NY.

Cade, T.J., Enderson, J. H., Thelander, C. G., White, C. M. (eds.). 1988. *Peregrine falcon populations their management and recovery*. The Peregrine Fund, Boise, Idaho.

Castagna, F., Montano, L., Lombardi, R., Pagano, A., Gigliotti, A., Bava, R., Lupia, C., Costagliola, A., Giordano, A., Palma, E., Britti, D., & Liguori, G. (2024). Understanding environmental contamination through the lens of the Peregrine Falcon (*Falco peregrinus*). Environments, 11(12), Article 12.

Caswell, H. 2001. *Matrix Population Models*. Sinauer Associates, Sunderland, Massachusetts.

Dorazio, R.M., Martin, J., Edwards, H.H. 2013. Estimating abundance while accounting for rarity, correlated behavior, and other sources of variation in counts. *Ecology*, 94, 1472–1478.

Gelman, A. 2005. Analysis of variance: Why is it more important than ever (with discussion). *Annals of Statistics*, 33, 1–53.

Greenwood, J.J.D. 2021. It was not DDT. *British Birds*, 114, 248–250.

Hefley, T.J., Broms, K.M., Brost, B.M., Buderman, F.E., Kay, S., Scharf, H.R., Tipton, J.R., Williams, P.J., Hooten, M.B. 2017. The basis function approach for modeling autocorrelation in ecological data. *Ecology*, 98, 632–646.

Hickey, J.J. 1969. *Peregrine Falcon populations: their biology and decline.* University of Wisconsin Press, Madison, Wisconsin.

Hickey, J.J., Anderson, D.W. 1968. Chlorinated hydrocarbons and eggshell changes in raptorial and fish-eating birds. *Science*, 162, 271–273.

Johnson, D.S., Hoeting, J.A. 2003. Autoregressive models for capture-recapture data: a Bayesian approach. *Biometrics*, 59, 341–350.

Kellner, K. 2024. *jagsUI: A wrapper around 'rjags' to streamline 'JAGS' analyses*. R package version 1.6.2.

Kéry, M., Royle, J.A. 2016. *AHM1—Modeling distribution, abundance and species richness using R and BUGS. Volume 1: Prelude and Static Models*. Elsevier, Academic Press.

Kéry, M., Royle, J.A. 2021. *AHM2—Modeling distribution, abundance and species richness using R and BUGS. Volume 2: Dynamic and Advanced Models*. Elsevier, Academic Press.

Kéry, M., Banderet, G., Müller, C., Pinaud, D., Savioz, J., Schmid, H., Werner, S., Monneret, R.-J. 2022. Spatio-temporal variation in post-recovery dynamics in a large Peregrine Falcon (*Falco peregrinus*) population in the Jura mountains 2000–2020. *Ibis*, 164, 217–239.

Koons, D.N., Arnold, T.W., Schaub, M. 2017. Understanding the demographic drivers of realized population growth rates. *Ecological Applications*, 27, 2102–2115.

Koons, D.N., Iles, D.T., Schaub, M., Caswell, H. 2016. A life-history perspective on the demographic drivers of structured population dynamics in changing environments. *Ecology Letters*, 19, 1023–1031.

Link, W.A., Barker, R.J. 2010. *Bayesian Inference with Ecological Applications*. Academic Press, London.

Mearns, R., Newton, I. 1984. Turnover and dispersal in a peregrine population. *Ibis*, 126, 347–355.

Monneret, R-J. 2017. *Le Faucon pèlerin*. Delachaux & Niestlé, Paris, France.

Monneret, R.-J., Ruffinoni, R., Parish, D., Pinaud, D., Kéry, M. 2019. The Peregrine population study in the French Jura mountains 1964–2016: use of occupancy modeling to estimate population size and analyze site persistence and colonization rates. *Ornis Hungarica*, 26, 69–90.

Newton, I. 1979. *Population ecology of raptors*. T. & A.D. Poyser, Calton, UK.

Newton I. 1998. *Population limitation in birds*. Academic Press, London.

Newton, I., Bogan, J.A., Haas, M.B. 1989. Organochlorines and mercury in the eggs of British Peregrines *Falco peregrinus*. *Ibis*, *131*, 355–376.

Oaks, J.L., Gilbert, M., Virani, M.Z., Watson, R.T., Meteyer, C.U., Rideout, B.A., Shivaprasad, H.L., Ahmed, S., Chaudhry, J.A., Arshad, M., Mahmood, S., Ali, A., Khan, A.A. 2004. Diclofenac residues as the cause of vulture population decline in Pakistan. *Nature*, 427, 631–633.

Oli, M.K., Smith, G.D., McGrady, M.J., Chaudhary, V., Rollie, C.J., Mearns, R., Newton, I., Lambin, X. 2023. Reproductive performance of Peregrine falcons relative to the use of organochlorine pesticides, 1946–2021. *Journal of Animal Ecology*, *92*, 2201–2213.

Plummer, M. 2003. JAGS: a program for analysis of Bayesian graphical models using Gibbs sampling. Proceedings of the 3rd International Workshop in Distributed Statistical Computing (DSC 2003) (eds K. Hornik, F. Leisch& A. Zeileis), 1–10, TU Vienna, Austria.

R Core Team. 2019. *R: A language and environment for statistical computing.* R Foundation for Statistical Computing, Vienna, Austria. https://www.R-project.org/

Ratcliffe, D.A. 1967. Decrease in eggshell weight in certain birds of prey. *Nature*, 215, 208–210.
Ratcliffe, D.A. 1970. Changes attributable to pesticides in egg breakage frequency and eggshell thickness in some British birds. *Journal of Applied Ecology*, 7, 67–115.
Ratcliffe, D.A. 1993. *The Peregrine Falcon*. T. & A.D. Poyser, Calton, UK.
Robinson, R.A., Grantham, M.J., Clark, J.A. 2009. Declining rates of ring recovery in British birds. *Ringing & Migration*, 24, 266–272.
Robinson, R.A., Wilson, M. 2021. Contrasting long-term trends in age-specific survival of Peregrine falcons (*Falco peregrinus*) in Britain using smoothed estimates of recovery probabilities. *Ibis*, 163, 890–898.
Schaub, M., Kéry, M. 2022. *Integrated Population Models — Theory and ecological applications with R and JAGS.* Elsevier, Academic Press.
Sibly, R.M., Newton, I., Walker, C.H. 2000. Effects of dieldrin on population growth rates of sparrowhawks 1963–1986. *Journal of Applied Ecology*, 37, 540–546.
Sielicki, T., Mizera, J. (eds). 2009. *Peregrine Falcon Populations: Status and Perspectives in the 21st Century.* Warsaw: Poznan University of Life Sciences Press.
Smith, G.D., Murillo-Garcia, O.E., Hostetler, J.A., Mearns, R., Rollie, C., Newton, I., McGrady, M.J., Oli, M.K. 2015. Demography of population recovery: Survival and fidelity of Peregrine falcons at various stages of population recovery. *Oecologia*, 178, 391–401.
Van Velzen, A.C., Stiles, W.B., Stickel, L.F. 1972. Lethal mobilization of DDT by cowbirds. *Journal of Wildlife Management*, 36, 733–739.
Wurster, D.H., Wurster, C.F. Jr., Strickland, W.N. 1965. Bird mortality following DDT spray for Dutch Elm disease. *Ecology*, 46, 488–499.

Figure legends

Fig. 1: Population size trajectories (number of pairs) of the peregrine falcon over 60 years (1964–2023) in the Swiss (left) and the French Jura study area (right). Note different scaling of the y axis.

Fig. 2: Estimates of demographic parameters under two IPMs with different formulations of random time effects in the demographic rates fit to the Swiss data only (posterior means and 95% CRIs): unstructured temporal random effects around a constant mean, leading to global smoothing (red), and random walk in time, leading to local smoothing; see text for more details.

Fig. 3: A closer look, for productivity, at the behavior of the two types of random-effects models in Fig. 2. Black symbols show the observed mean annual brood size, with size proportional to sample size in terms of the number of broods. Red and blue polygons show 95% CRIs from two simplified versions of the two models in Fig. 2c with a single productivity parameter. Red and blue lines show predictions from a linear model fit to productivity data alone, with either a constant or with a smoothing spline of year.

Fig. 4: Estimates of demographic parameters under the IPMs with random walk in time for demographic parameters, fit to the Swiss and French data combined (posterior means and 95% CRIs).

Fig. 5: Posterior distribution of the difference in adult survival probability between the start of the study (1964) and the year with highest estimated adult survival (1978).

Fig. 6: Relative contributions of different demographic parameters and of population structure to the realized population growth rate from a retrospective analysis (tLTRE).

Figure 1

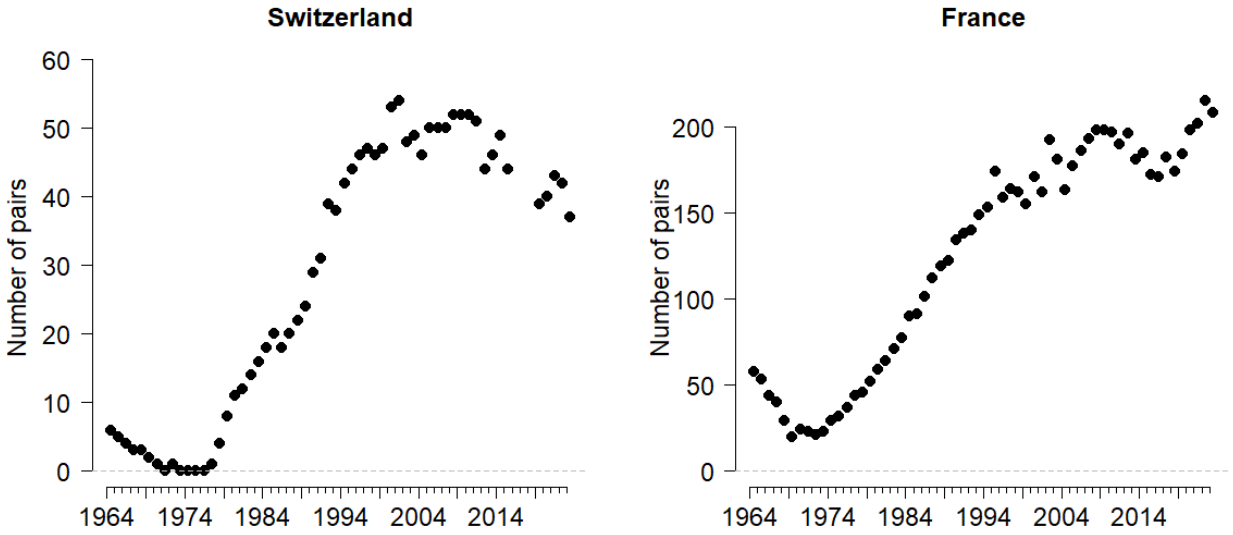

Switzerland
France
Number of pairs
Number of pairs
0
10
20
30
40
50
60
0
50
100
150
200
1964
1974
1984
1994
2004
2014

Figure 2

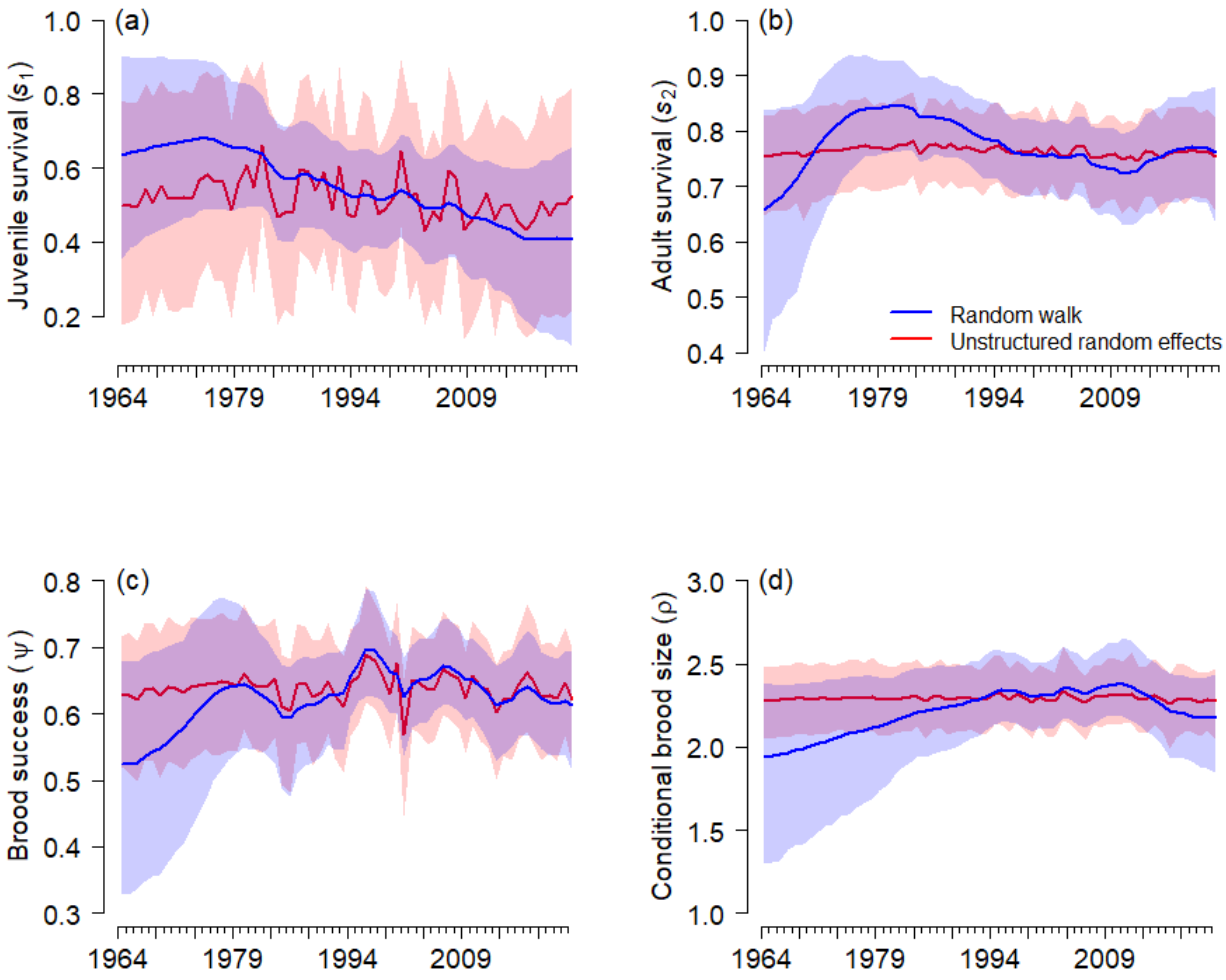

(a)
Juvenile survival (s_1)
1.0
0.8
0.6
0.4
0.2
1964
1979
1994
2009
(b)
Adult survival (s_2)
1.0
0.9
0.8
0.7
0.6
0.5
0.4
Random walk
Unstructured random effects
(c)
Brood success (ψ)
0.8
0.7
0.6
0.5
0.4
0.3
(d)
Conditional brood size (ρ)
3.0
2.5
2.0
1.5
1.0

Figure 3

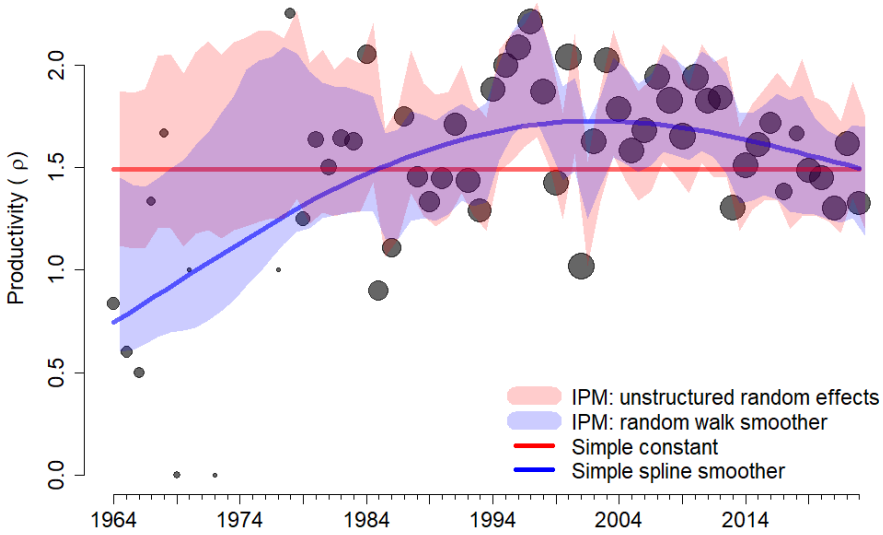

Productivity (ρ)
0.0
0.5
1.0
1.5
2.0
1964
1974
1984
1994
2004
2014
IPM: unstructured random effects
IPM: random walk smoother
Simple constant
Simple spline smoother

Figure 4

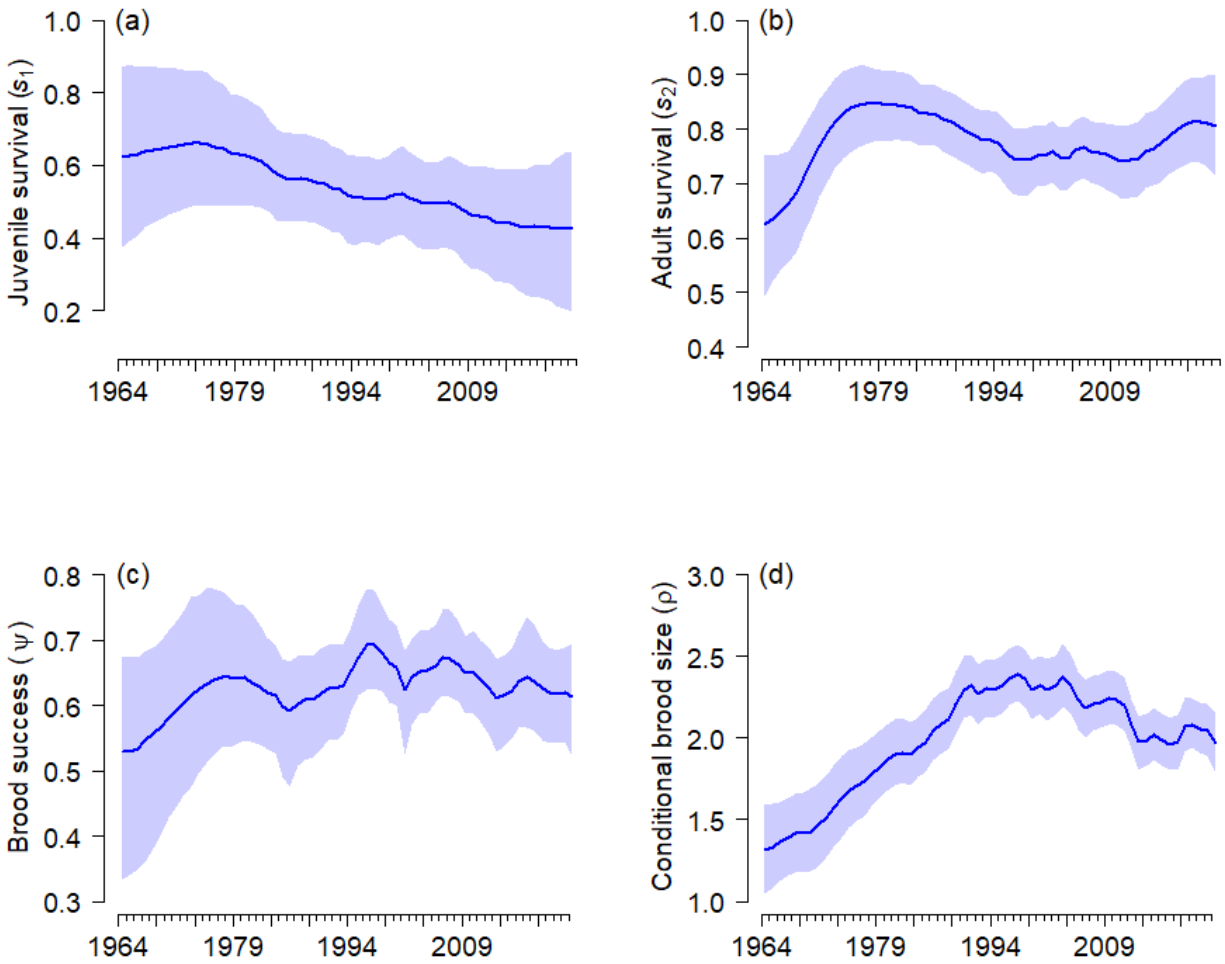

(a)
Juvenile survival (s_1)
1.0
0.8
0.6
0.4
0.2
1964
1979
1994
2009
(b)
Adult survival (s_2)
1.0
0.9
0.8
0.7
0.6
0.5
0.4
1964
1979
1994
2009
(c)
Brood success (ψ)
0.8
0.7
0.6
0.5
0.4
0.3
1964
1979
1994
2009
(d)
Conditional brood size (ρ)
3.0
2.5
2.0
1.5
1.0
1964
1979
1994
2009

Figure 5

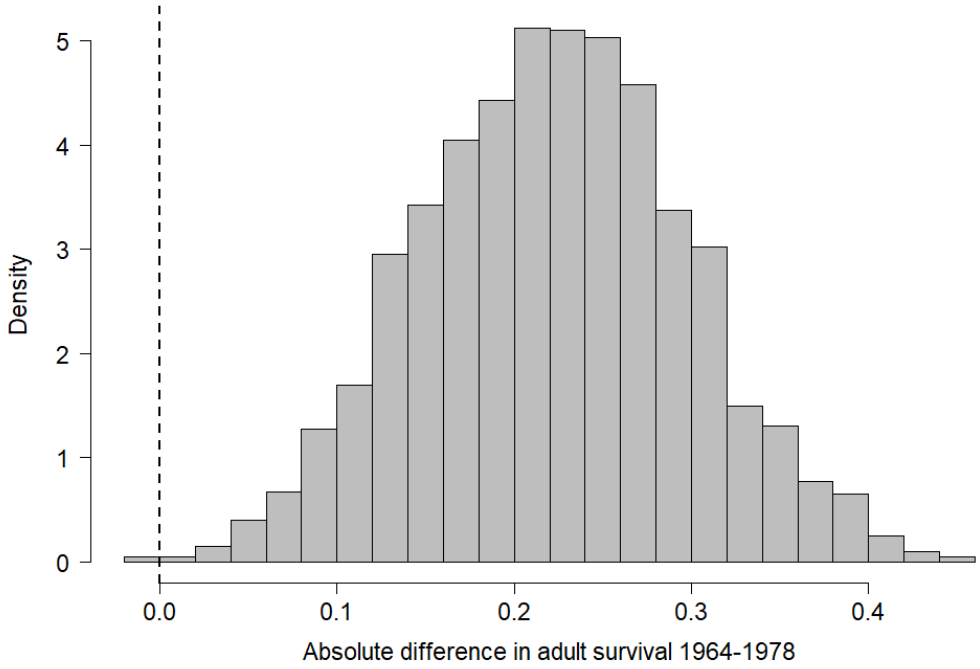
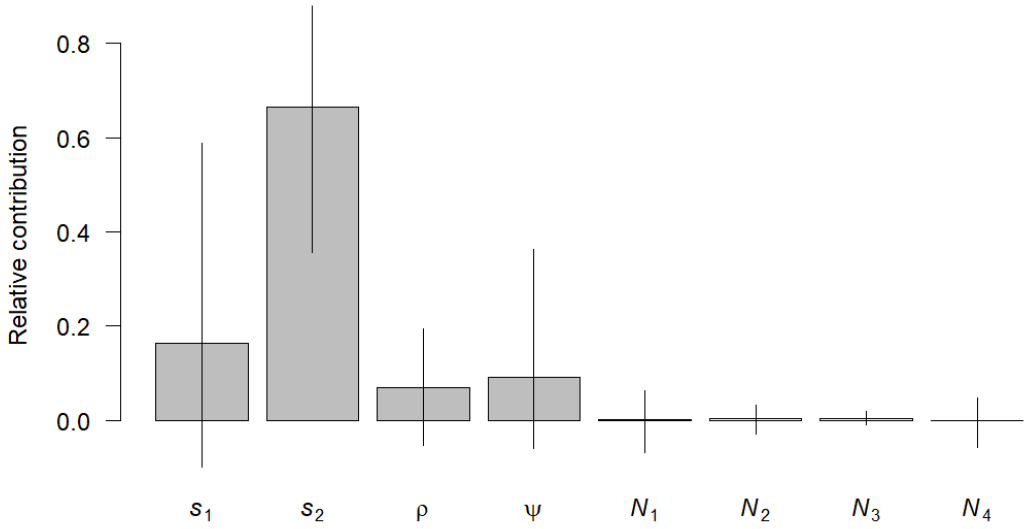

Density
0
1
2
3
4
5
0.0
0.1
0.2
0.3
0.4
Absolute difference in adult survival 1964-1978

Figure 6



Supporting Information

Marc Kéry, René-Jean Monneret, Jaume A. Badia-Boher, Michael Schaub: Demographic causes of the pesticide crash in the peregrine falcon.

Appendix S1: Map of the study area, showing the French Jura in blue and the Southern Swiss Jura with adjacent areas in red.

Appendix S2: Frequency distribution of the annual number of ringed peregrines in the Swiss study area.

Appendix S3: Life cycle graph of the Markovian model of population dynamics of peregrines in the Jura mountains. Parameter θ is the unconditional brood size, i.e., the number of young regardless of whether a brood was successful or not. We expressed it according to a hurdle model as a function of brood success (ψ) and conditional brood size (ρ); see main text for more details.

Appendix S4: Overview of the data, and representation of the population model fitted as an IPM in the BUGS language as implemented in software JAGS.

Appendix S5: Posterior predictive check of the goodness of fit of the model to the observed data, conducted within a single model run but separately for each response variable.

Appendix S6: Comparison of the estimates of the logistic regression on year of recovery probability under the traditional random effects model with unstructured time effects around a constant mean, and under a random walk model, respectively, in the demographic rates fit to the Swiss data only (posterior means and 95% CRIs shown): red: unstructured temporal random effects; blue: random walk in time.

Appendix S7: Posterior summary of the parameters of the IPM with autoregressive random effects of time fit to the peregrine data sets from both the French and the Swiss study areas (i.e., the model shown in Appendix S3).

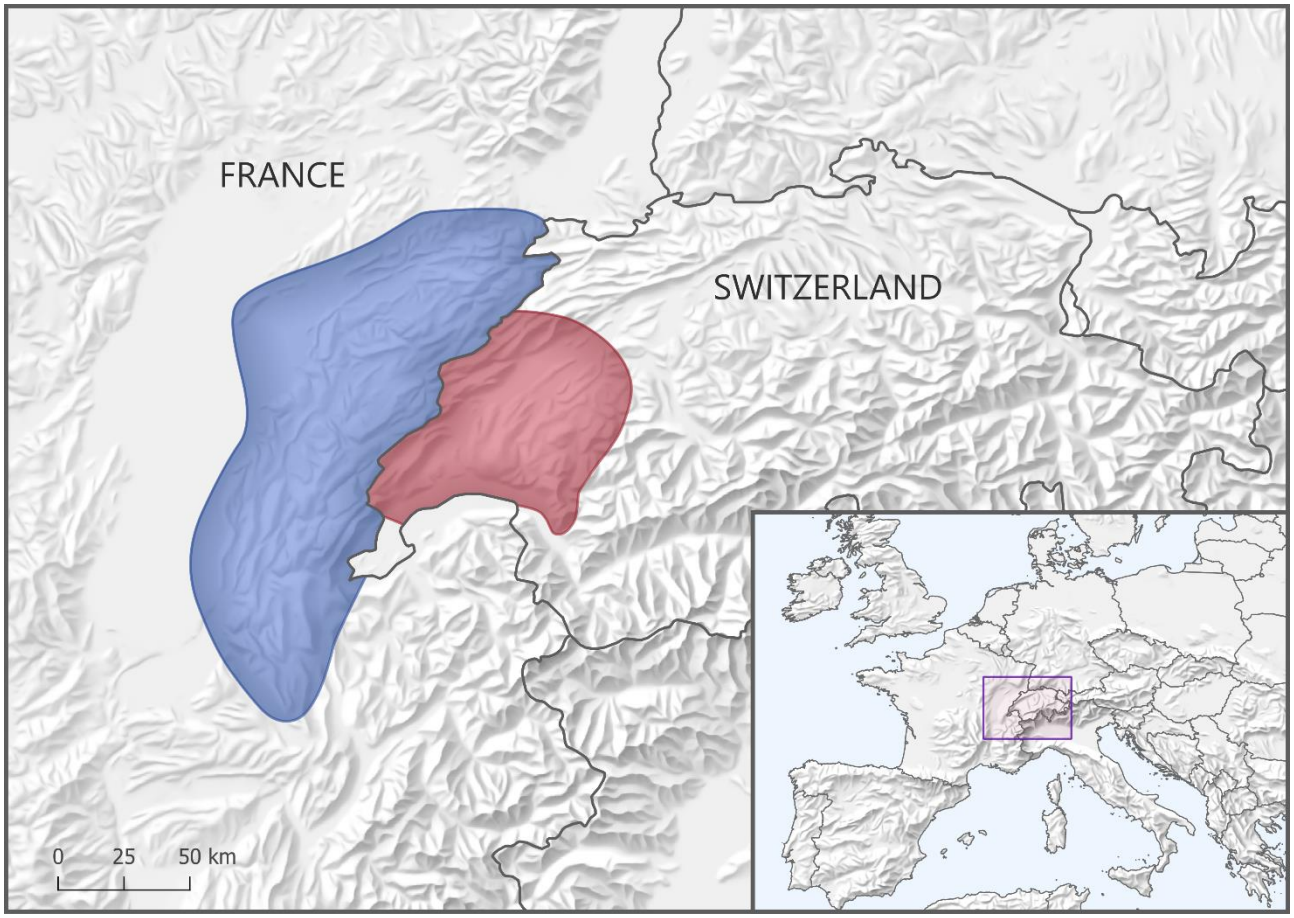
Appendix S8: Prior sensitivity analysis of the main result of our study, the increase in adult survival during the early years of the study, i.e., during the pesticide crash, under multiple assumed priors for survival probability during the first interval (1964–1965)

Appendix S9: Estimated trajectories of the number of breeding pairs in the Swiss and the French long-term study (posterior means with 95% CRIs). Red symbols show the observed counts of territorial pairs. Note different scaling of the y-axis.

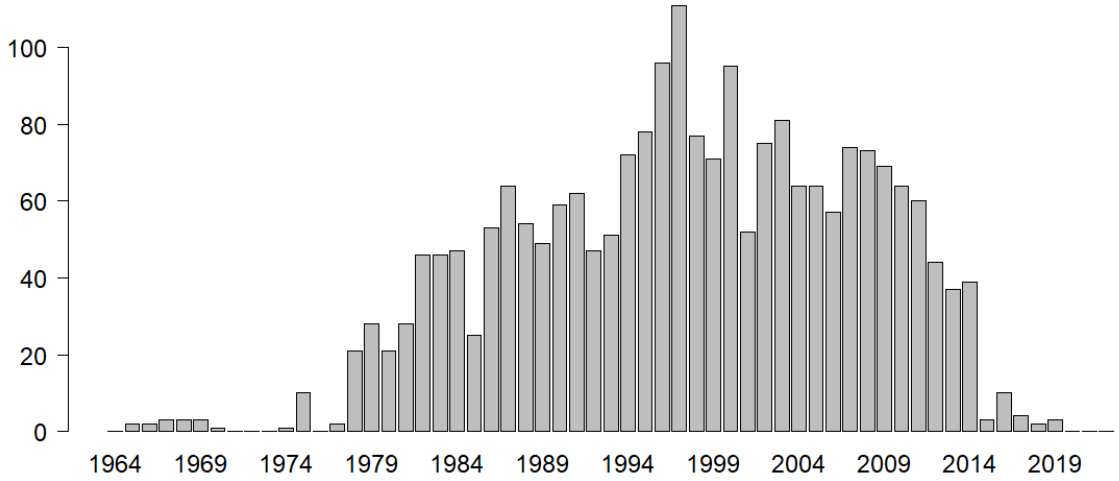
Appendix S10: Stage distributions of the population, and proportion of floaters, in the Swiss study area under the random-walk model fit to the data from both study areas.

Appendix S11: Stage distributions of the population, and proportion of floaters, in the French study area under the random-walk model fit to the data from both study areas.

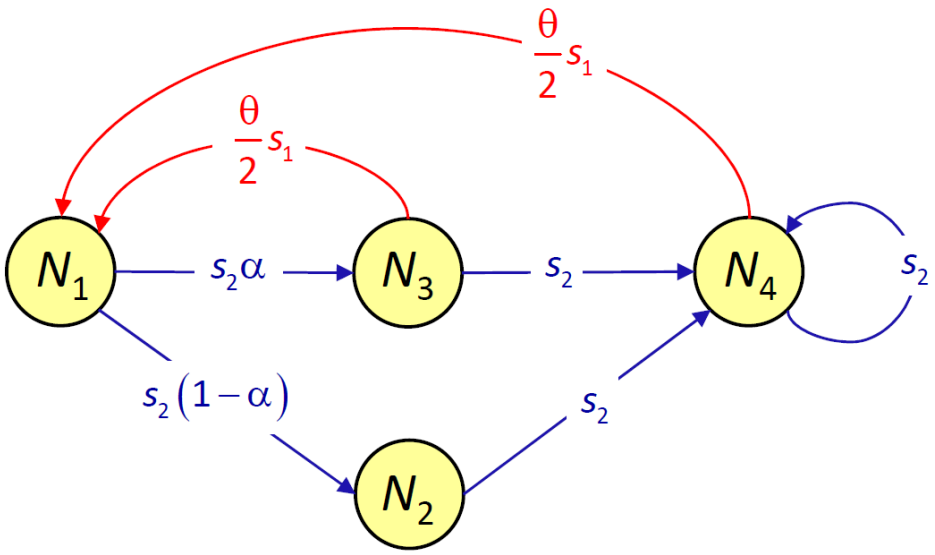
Appendix S1: Map of the study area, showing the French Jura in blue and the Southern Swiss Jura with adjacent areas in red.



Appendix S2: Frequency distribution of the annual number of ringed peregrines in the Swiss study area.



Appendix S3: Life cycle graph of the Markovian model of population dynamics of peregrines in the Jura mountains, where pure survival transitions are depicted in blue and transitions involving reproduction in red. Parameter θ is the unconditional brood size, i.e., the number of young regardless of whether a brood was successful or not. We used a hurdle model to decompose θ into brood success probability (ψ) and conditional brood size (ρ); see text for more details. Conditional brood size was stratified by study area (i.e., French and Swiss Jura), while all other models in the graph were shared among the two studies.



Appendix S4: Overview of the data, and representation of the population model fitted as an IPM in the BUGS language as implemented in software JAGS.

Overview of the data:

```
List of 15
 $ nyears   : int 60
 $ marr     : num [1:59, 1:60] 0 0 0 0 0 0 0 0 0 0 ...
  ..- attr(*, "dimnames")=List of 2
  .. ..$ released : chr [1:59] "Y1" "Y2" "Y3" "Y4" ...
  .. ..$ recovered: chr [1:60] "Y2" "Y3" "Y4" "Y5" ...
 $ rel      : Named num [1:59] 0 2 2 3 3 3 1 0 0 0 ...
  ..- attr(*, "names")= chr [1:59] "Y1" "Y2" "Y3" "Y4" ...
 $ yCH      : Named int [1:60] 6 5 4 3 3 2 1 0 1 0 ...
  ..- attr(*, "names")= chr [1:60] "1964" "1965" "1966" "1967" ...
 $ nBroodsCH: int 1663
 $ goodCH   : num [1:1663] 0 0 0 1 1 1 0 0 0 1 ...
 $ nYoungCH : num [1:1663] 0 0 0 1 2 2 0 0 0 1 ...
 $ YrCH     : int [1:1663] 1 1 1 1 1 1 2 2 2 2 ...
 $ zeroes   : num [1:1663] 0 0 0 0 0 0 0 0 0 0 ...
 $ pNinitCH : num [1:10] 0.1 0.1 0.1 0.1 0.1 0.1 0.1 0.1 0.1 0.1
 $ yF       : Named num [1:60] 58 53 44 40 29 20 24 23 21 23 ...
  ..- attr(*, "names")= chr [1:60] "1964" "1965" "1966" "1967" ...
 $ nBroodsF : int 4124
 $ nYoungF  : num [1:4124] 1 1 1 1 1 1 1 2 2 1 ...
 $ YrF      : int [1:4124] 1 1 1 1 1 1 1 1 1 2 ...
 $ pNinitF  : num [1:50] 0.02 0.02 0.02 0.02 0.02  ...
```

BUGS language representation of the model with temporal autocorrelation in demographic rates:

```
cat(file = "model11D.txt", "
model {

  # Priors and linear models

  # Parameter model in year/interval 1
  # Survival (shared among data sets)
  for (a in 1:2){                  # Loop over 2 age classes
    s[a,1] ~ dunif(0, 1)           # Prior of survival in year 1
    logit.s[a,1] <- logit(s[a,1])
  }
  # Productivity rate (separate between data sets)
  rhoCH[1] ~ dnorm(0, 1)T(0,)  # Prior of productivity in year 1 CH
  log.rhoCH[1] <- log(rhoCH[1])
# curve(dnorm(x, 0, 1), 0, 3)
  rhoF[1] ~ dnorm(0, 1)T(0,)   # Prior of productivity in year 1 F
```

```
  log.rhoF[1] <- log(rhoF[1])

  # Autoregressive parameter model in later years/intervals
  # Autoregressive models for survival (shared)
  for (a in 1:2){                 # Loop over 2 age classes
    for (t in 2:(nyears-1)){
      logit.s[a,t] ~ dnorm(logit.s[a,t-1], tau.s[a])
      s[a,t] <- ilogit(logit.s[a,t])
    }
    sigma.s[a] ~ dnorm(0, 1)T(0,)
    # curve(dnorm(x, 0, sqrt(1/10)), 0, 1)
    tau.s[a] <- pow(sigma.s[a], -2)
  }

  # Autoregressive model for rhoCH and rhoF (separate)
  for (t in 2:nyears){
    log.rhoCH[t] ~ dnorm(log.rhoCH[t-1], tau.rhoCH)
    rhoCH[t] <- exp(log.rhoCH[t])
    log.rhoF[t] ~ dnorm(log.rhoF[t-1], tau.rhoF)
    rhoF[t] <- exp(log.rhoF[t])
  }
  sigma.rhoCH ~ dnorm(0, 1)T(0,)
  tau.rhoCH <- pow(sigma.rhoCH, -2)
  sigma.rhoF ~ dnorm(0, 1)T(0,)
  tau.rhoF <- pow(sigma.rhoF, -2)


  # Modell for brood success (for variable 'goodCH'; shared)
  psi[1] ~ dunif(0, 1)      # Prior of success in year 1
  logit.psi[1] <- logit(psi[1])
  for (t in 2:nyears){      # Autoregressive model for psi
    logit.psi[t] ~ dnorm(logit.psi[t-1], tau.psi)
    psi[t] <- ilogit(logit.psi[t])
  }
  sigma.psi ~ dnorm(0, 1)T(0,)
  tau.psi <- pow(sigma.psi, -2)


  # Model for alpha (shared)
  alpha ~ dbeta(1, 1)  # Prior for prob. start repro. at age 2y

  # Model for r
  for (t in 1:(nyears-1)){
    logit(r[t]) <- beta[1]+beta[2]*((t-30)/29) # Trend in recovery
  }
  for (i in 1:2){              # Priors for betas (recovery
regression)
    beta[i] ~ dnorm(0, 0.1)
  }


  # Prior for observation model (separate among data sets)
  tau.epsCH <- pow(sigma.epsCH, -2)
  sigma.epsCH ~ dnorm(0, 1)T(0.001,)
  tau.epsF <- pow(sigma.epsF, -2)
  sigma.epsF ~ dnorm(0, 1)T(0.001,)
```

```
  # Population count data:
  #   State-space model with matrix population state model

  # Population model (state): separate among data sets
  # Model for the initial population size: discrete uniform priors
  for (a in 1:4){
    NCH[a,1] ~ dcat(pNinitCH)
    NF[a,1] ~ dcat(pNinitF)
  }

  # Process model over time: our model of population dynamics
(state):
  #   Separate among data sets
  for (t in 1:(nyears-1)){
    # 1-year-old birds (non-breeding): note psi is shared
    rhoHurdleCH[t] <- (psi[t] / (1-exp(-rhoCH[t]))) * rhoCH[t]
    rhoHurdleF[t] <- (psi[t] / (1-exp(-rhoF[t]))) * rhoF[t]
    NCH[1,t+1] ~ dpois(rhoHurdleCH[t]/2 * s[1,t] *
(NCH[3,t]+NCH[4,t]))
    NF[1,t+1] ~ dpois(rhoHurdleF[t]/2* s[1,t] * (NF[3,t]+NF[4,t]))

    # 2-year-old birds (non-breeding)
    NCH[2,t+1] ~ dbin(s[2,t] * (1-alpha), NCH[1,t])
    NF[2,t+1] ~ dbin(s[2,t] * (1-alpha), NF[1,t])

    # 2-year-old birds (first-time breeders)
    NCH[3,t+1] ~ dbin(s[2,t] * alpha, NCH[1,t])
    NF[3,t+1] ~ dbin(s[2,t] * alpha, NF[1,t])

    # 3-year-old and older birds (breeding)
    NCH[4,t+1] ~ dbin(s[2,t], (NCH[2,t] + NCH[3,t] + NCH[4,t]))
    NF[4,t+1] ~ dbin(s[2,t], (NF[2,t] + NF[3,t] + NF[4,t]))
  }

  # Observation model for 1964-2023: Poisson log-normal
  #   Separate among data sets
  for (t in 1:nyears){
    NBCH[t] <- NCH[3,t] + NCH[4,t] # Calculate number of breeding
pairs
    yCH[t] ~ dpois(NBCH[t] * exp(epsCH[t])) # PLN error Switzerland
    NBF[t] <- NF[3,t] + NF[4,t]
    yF[t] ~ dpois(NBF[t] * exp(epsF[t]))    # PLN error France

    # Define random effects for PLN Switzerland and France
    epsCH[t] ~ dnorm(0, tau.epsCH)
    epsF[t] ~ dnorm(0, tau.epsF)

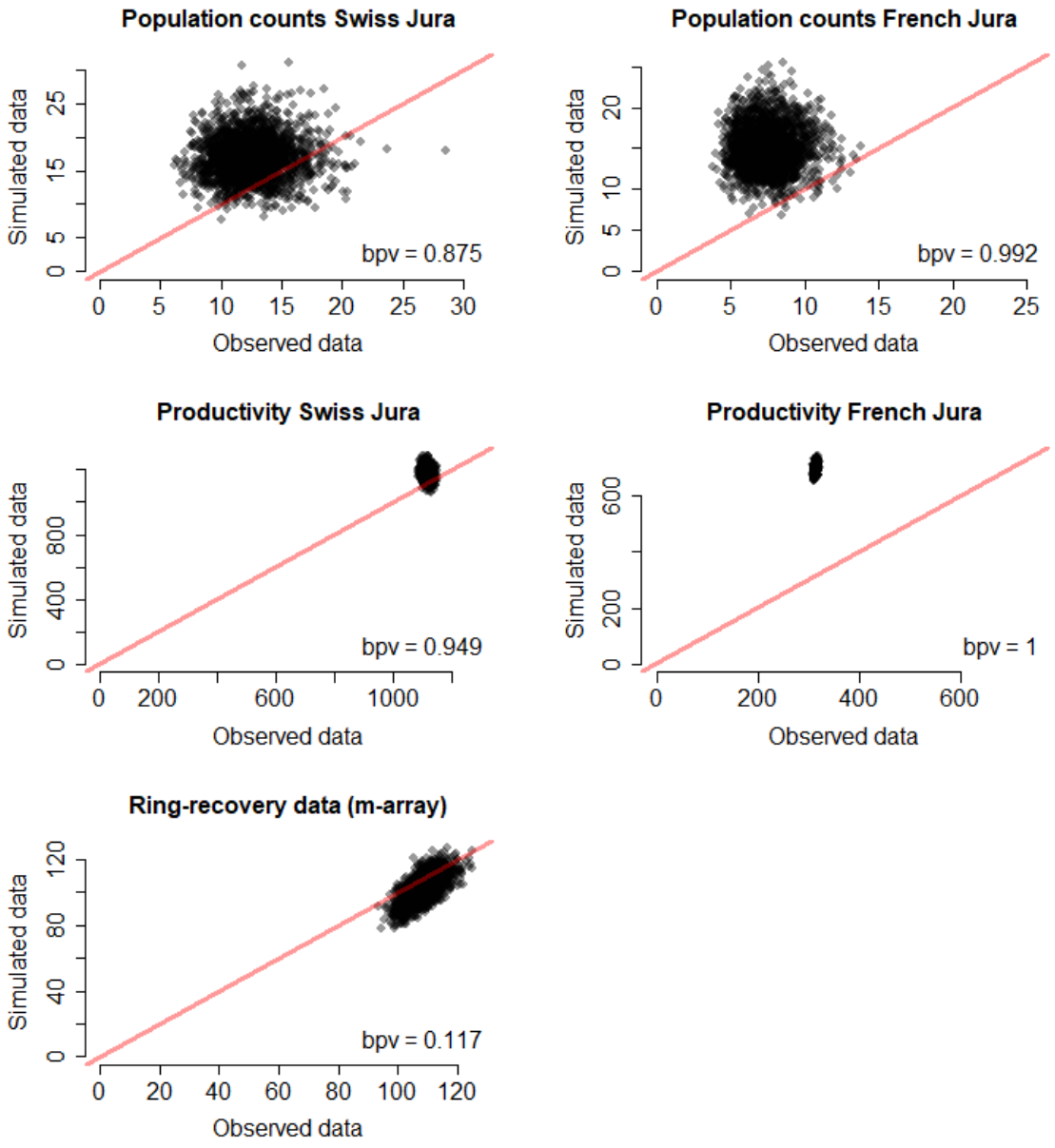
    # Compute expected value for counts
    E_NBCH[t] <- NBCH[t] * exp(pow(sigma.epsCH,2)/2)
    E_NBF[t] <- NBF[t] * exp(pow(sigma.epsF,2)/2)
  }

  # Dead-recovery data: multinomial ring-recovery model
  #   Shared among the two regions
  # Define the multinomial likelihood
```

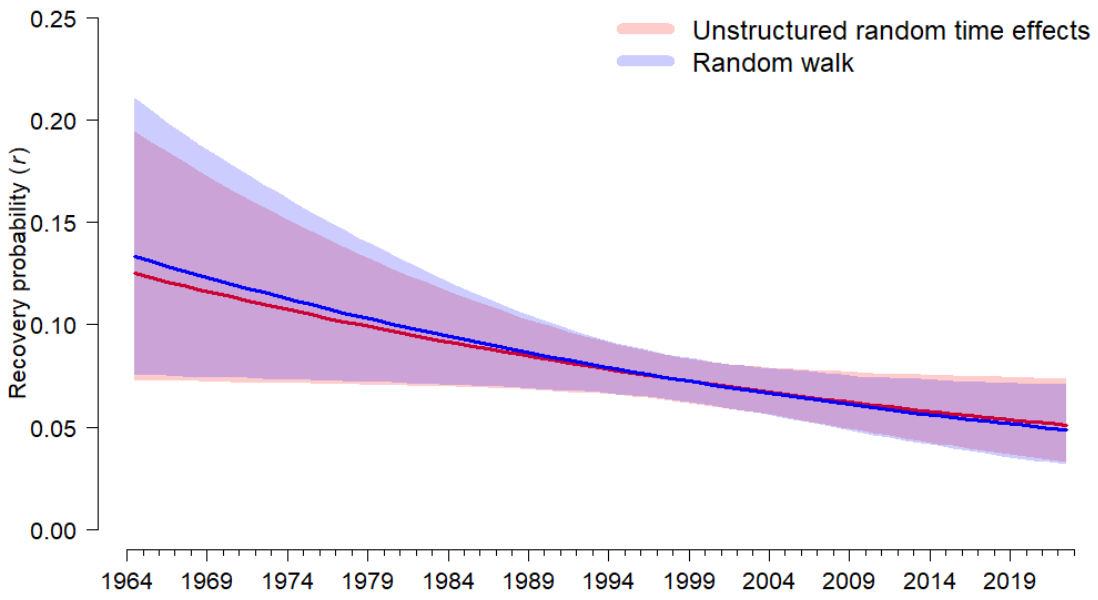
```
  for (t in 1:(nyears-1)){
    marr[t,1:nyears] ~ dmulti(pr[t,], rel[t])
  }
  # Define the cell probabilities of the m-array
  for (t in 1:(nyears-1)){
    # Main diagonal
    pr[t,t] <- (1-s[1,t]) * r[t]
    # Above main diagonal
    for (j in (t+2):(nyears-1)){
      pr[t,j] <- s[1,t] * prod(s[2,(t+1):(j-1)]) * (1-s[2,j]) * r[j]
    } #j
    # Below main diagonal
    for (j in 1:(t-1)){
      pr[t,j] <- 0
    } #j
  } #t
  # One above main diagonal
  for (t in 1:(nyears-2)){
    pr[t,t+1] <- s[1,t] * (1-s[2,t+1]) * r[t+1]
  } #t
  # Last column: probability of non-recovery
  for (t in 1:(nyears-1)){
    pr[t,nyears] <- 1-sum(pr[t,1:(nyears-1)])
  } #t

  # Productivity data: Poisson regression
  # Switzerland: Hurdle Poisson
  for (i in 1:nBroodsCH){
    zeroes[i] ~ dpois(-ll[i] + 10000)
    tPois[i] <- log(exp(-rhoCH[YrCH[i]]) * pow(rhoCH[YrCH[i]],
nYoungCH[i]) / exp(logfact(nYoungCH[i])) / (1-exp(-rhoCH[YrCH[i]])))
    l1[i] <- (1-goodCH[i]) * log(1-psi[YrCH[i]])
    l2[i] <- goodCH[i] * (log(psi[YrCH[i]]) + tPois[i])
    ll[i] <- l1[i] + l2[i]
  }
  # France: zero-truncated Poisson
  for (i in 1:nBroodsF){
    nYoungF[i] ~ dpois(rhoF[YrF[i]])T(1,)
  }
}
")
```

Appendix S5: Posterior predictive check of the goodness of fit of the model to the observed data, conducted within a single model run but separately for each response variable. Graphs show the summed values of a Freeman-Tukey discrepancy measure for data simulated under the model on the y-axis against those when computed for the actual data in the analysis on the x-axis. The value of the Bayesian p-value (bpv) is shown in each panel and corresponds to the proportion of MCMC draws that lie above the red 1:1 line.



Appendix S6: Comparison of the estimates of the logistic regression on year of recovery probability under the traditional random effects model with unstructured time effects around a constant mean, and under a random walk model, respectively, in the demographic rates fit to the Swiss data only (posterior means and 95% CRIs shown): red: global smoothing by unstructured temporal random effects around a constant mean; blue: local smoothing by a random walk in time.



Appendix S7: Posterior summary of the parameters of the IPM with autoregressive random effects of time fit to the peregrine data sets from both the French and the Swiss study areas (i.e., the model shown in Appendix S3). The four columns give the posterior mean and posterior standard deviation and the 2.5 and 97.5 percentiles of the posterior distribution.

	mean	sd	2.5%	97.5%
alpha	0.373	0.2284	0.0294	0.862
beta[1]	-2.453	0.0929	-2.6391	-2.279
beta[2]	-0.510	0.2383	-0.9782	-0.035
sigma.s[1]	0.139	0.0861	0.0192	0.357
sigma.s[2]	0.159	0.0477	0.0801	0.262
sigma.psi	0.127	0.0745	0.0083	0.287
sigma.rhoCH	0.030	0.0186	0.0025	0.073
sigma.epsCH	0.028	0.0213	0.0020	0.081
sigma.rhoF	0.051	0.0132	0.0298	0.081
sigma.epsF	0.014	0.0104	0.0013	0.041
s[1,1]	0.617	0.1249	0.3600	0.867
s[2,1]	0.624	0.0675	0.4891	0.750
s[1,2]	0.619	0.1220	0.3834	0.870
s[2,2]	0.635	0.0588	0.5195	0.748
s[1,3]	0.623	0.1198	0.3853	0.869
s[2,3]	0.649	0.0561	0.5356	0.755
s[1,4]	0.630	0.1164	0.4076	0.861
s[2,4]	0.662	0.0545	0.5523	0.765
s[1,5]	0.636	0.1119	0.4367	0.862
s[2,5]	0.685	0.0521	0.5732	0.780
s[1,6]	0.643	0.1095	0.4505	0.871
s[2,6]	0.713	0.0486	0.6134	0.802
s[1,7]	0.648	0.1072	0.4625	0.870
s[2,7]	0.743	0.0464	0.6433	0.829
s[1,8]	0.652	0.1040	0.4698	0.867
s[2,8]	0.769	0.0440	0.6812	0.853
s[1,9]	0.655	0.1023	0.4757	0.869
s[2,9]	0.793	0.0435	0.7047	0.876
s[1,10]	0.657	0.1002	0.4843	0.867
s[2,10]	0.813	0.0423	0.7293	0.892
s[1,11]	0.657	0.0972	0.4833	0.859
s[2,11]	0.828	0.0404	0.7481	0.903
s[1,12]	0.655	0.0950	0.4844	0.844
s[2,12]	0.838	0.0390	0.7594	0.907
s[1,13]	0.649	0.0921	0.4848	0.842
s[2,13]	0.844	0.0378	0.7667	0.914
s[1,14]	0.642	0.0891	0.4884	0.830
s[2,14]	0.847	0.0364	0.7723	0.913
s[1,15]	0.631	0.0823	0.4857	0.805
s[2,15]	0.846	0.0357	0.7740	0.914
s[1,16]	0.627	0.0803	0.4857	0.789
s[2,16]	0.845	0.0352	0.7695	0.910
s[1,17]	0.624	0.0784	0.4872	0.789
s[2,17]	0.844	0.0333	0.7756	0.905
s[1,18]	0.616	0.0753	0.4844	0.777
s[2,18]	0.844	0.0331	0.7764	0.905
s[1,19]	0.610	0.0713	0.4832	0.761

s[2,19]	0.842	0.0324	0.7769	0.901
s[1,20]	0.590	0.0646	0.4692	0.724
s[2,20]	0.838	0.0305	0.7777	0.896
s[1,21]	0.574	0.0653	0.4418	0.702
s[2,21]	0.828	0.0299	0.7694	0.881
s[1,22]	0.564	0.0645	0.4310	0.690
s[2,22]	0.828	0.0289	0.7693	0.883
s[1,23]	0.560	0.0634	0.4380	0.685
s[2,23]	0.826	0.0286	0.7679	0.879
s[1,24]	0.563	0.0621	0.4498	0.690
s[2,24]	0.820	0.0287	0.7600	0.871
s[1,25]	0.559	0.0602	0.4504	0.686
s[2,25]	0.814	0.0294	0.7534	0.868
s[1,26]	0.552	0.0582	0.4411	0.674
s[2,26]	0.804	0.0290	0.7433	0.858
s[1,27]	0.547	0.0581	0.4386	0.669
s[2,27]	0.797	0.0281	0.7394	0.851
s[1,28]	0.536	0.0576	0.4262	0.659
s[2,28]	0.787	0.0287	0.7262	0.840
s[1,29]	0.532	0.0589	0.4165	0.650
s[2,29]	0.781	0.0287	0.7214	0.835
s[1,30]	0.519	0.0604	0.3934	0.636
s[2,30]	0.780	0.0288	0.7210	0.834
s[1,31]	0.512	0.0619	0.3740	0.629
s[2,31]	0.774	0.0290	0.7194	0.830
s[1,32]	0.510	0.0606	0.3826	0.623
s[2,32]	0.758	0.0299	0.6974	0.815
s[1,33]	0.509	0.0585	0.3828	0.623
s[2,33]	0.749	0.0310	0.6835	0.807
s[1,34]	0.506	0.0588	0.3855	0.614
s[2,34]	0.744	0.0309	0.6781	0.800
s[1,35]	0.510	0.0578	0.3935	0.622
s[2,35]	0.745	0.0309	0.6829	0.800
s[1,36]	0.518	0.0587	0.3996	0.637
s[2,36]	0.752	0.0296	0.6889	0.807
s[1,37]	0.524	0.0611	0.4067	0.656
s[2,37]	0.751	0.0295	0.6897	0.808
s[1,38]	0.511	0.0610	0.3899	0.631
s[2,38]	0.759	0.0293	0.7004	0.817
s[1,39]	0.502	0.0603	0.3788	0.616
s[2,39]	0.749	0.0303	0.6837	0.804
s[1,40]	0.495	0.0593	0.3753	0.607
s[2,40]	0.747	0.0302	0.6812	0.804
s[1,41]	0.494	0.0603	0.3740	0.608
s[2,41]	0.761	0.0292	0.7023	0.818
s[1,42]	0.495	0.0619	0.3734	0.613
s[2,42]	0.765	0.0306	0.7043	0.824
s[1,43]	0.499	0.0645	0.3763	0.627
s[2,43]	0.759	0.0300	0.6971	0.815
s[1,44]	0.493	0.0676	0.3609	0.632
s[2,44]	0.756	0.0299	0.6974	0.815
s[1,45]	0.476	0.0705	0.3307	0.609
s[2,45]	0.753	0.0313	0.6894	0.813
s[1,46]	0.466	0.0743	0.3102	0.601
s[2,46]	0.749	0.0321	0.6859	0.811
s[1,47]	0.460	0.0780	0.2993	0.606

s[2,47]	0.743	0.0335	0.6772	0.807
s[1,48]	0.455	0.0789	0.2923	0.599
s[2,48]	0.745	0.0340	0.6763	0.811
s[1,49]	0.445	0.0814	0.2800	0.593
s[2,49]	0.747	0.0348	0.6745	0.814
s[1,50]	0.441	0.0832	0.2729	0.593
s[2,50]	0.760	0.0340	0.6957	0.826
s[1,51]	0.438	0.0853	0.2613	0.595
s[2,51]	0.766	0.0359	0.6928	0.836
s[1,52]	0.431	0.0908	0.2437	0.597
s[2,52]	0.775	0.0361	0.7017	0.845
s[1,53]	0.428	0.0914	0.2444	0.592
s[2,53]	0.787	0.0365	0.7183	0.859
s[1,54]	0.430	0.0945	0.2357	0.603
s[2,54]	0.798	0.0381	0.7270	0.874
s[1,55]	0.431	0.0989	0.2284	0.618
s[2,55]	0.807	0.0390	0.7351	0.888
s[1,56]	0.429	0.1033	0.2152	0.618
s[2,56]	0.813	0.0404	0.7357	0.897
s[1,57]	0.428	0.1077	0.1961	0.631
s[2,57]	0.813	0.0416	0.7310	0.896
s[1,58]	0.427	0.1129	0.1889	0.635
s[2,58]	0.809	0.0445	0.7251	0.902
s[1,59]	0.427	0.1180	0.1777	0.652
s[2,59]	0.803	0.0487	0.7078	0.899
psi[1]	0.526	0.0959	0.3132	0.679
psi[2]	0.525	0.0952	0.3157	0.672
psi[3]	0.529	0.0926	0.3281	0.680
psi[4]	0.541	0.0872	0.3541	0.684
psi[5]	0.553	0.0814	0.3784	0.685
psi[6]	0.563	0.0784	0.3919	0.688
psi[7]	0.578	0.0756	0.4101	0.703
psi[8]	0.591	0.0731	0.4384	0.722
psi[9]	0.603	0.0710	0.4531	0.741
psi[10]	0.616	0.0689	0.4684	0.756
psi[11]	0.626	0.0686	0.4855	0.774
psi[12]	0.634	0.0666	0.5029	0.782
psi[13]	0.641	0.0656	0.5140	0.784
psi[14]	0.646	0.0634	0.5291	0.786
psi[15]	0.647	0.0585	0.5369	0.778
psi[16]	0.647	0.0552	0.5418	0.766
psi[17]	0.647	0.0519	0.5518	0.761
psi[18]	0.639	0.0484	0.5464	0.740
psi[19]	0.630	0.0453	0.5369	0.721
psi[20]	0.622	0.0419	0.5354	0.704
psi[21]	0.614	0.0416	0.5277	0.693
psi[22]	0.596	0.0464	0.4873	0.670
psi[23]	0.591	0.0484	0.4784	0.666
psi[24]	0.604	0.0417	0.5116	0.677
psi[25]	0.609	0.0411	0.5118	0.681
psi[26]	0.610	0.0396	0.5232	0.678
psi[27]	0.616	0.0368	0.5367	0.682
psi[28]	0.626	0.0344	0.5539	0.689
psi[29]	0.627	0.0337	0.5525	0.687
psi[30]	0.630	0.0343	0.5561	0.691
psi[31]	0.653	0.0312	0.5903	0.719

psi[32]	0.674	0.0347	0.6170	0.748
psi[33]	0.693	0.0418	0.6268	0.782
psi[34]	0.693	0.0401	0.6283	0.778
psi[35]	0.681	0.0350	0.6209	0.753
psi[36]	0.664	0.0313	0.6065	0.729
psi[37]	0.659	0.0304	0.6025	0.720
psi[38]	0.625	0.0403	0.5299	0.689
psi[39]	0.644	0.0318	0.5736	0.704
psi[40]	0.653	0.0307	0.5895	0.713
psi[41]	0.655	0.0311	0.5914	0.713
psi[42]	0.661	0.0314	0.6009	0.725
psi[43]	0.674	0.0339	0.6171	0.746
psi[44]	0.672	0.0330	0.6158	0.743
psi[45]	0.664	0.0315	0.6087	0.731
psi[46]	0.649	0.0300	0.5878	0.710
psi[47]	0.650	0.0315	0.5903	0.719
psi[48]	0.639	0.0300	0.5768	0.697
psi[49]	0.627	0.0323	0.5567	0.687
psi[50]	0.613	0.0362	0.5308	0.672
psi[51]	0.616	0.0354	0.5365	0.678
psi[52]	0.623	0.0339	0.5502	0.686
psi[53]	0.637	0.0362	0.5672	0.716
psi[54]	0.644	0.0401	0.5722	0.732
psi[55]	0.638	0.0388	0.5638	0.722
psi[56]	0.624	0.0365	0.5473	0.698
psi[57]	0.617	0.0351	0.5453	0.683
psi[58]	0.614	0.0366	0.5383	0.683
psi[59]	0.619	0.0374	0.5398	0.689
psi[60]	0.611	0.0429	0.5141	0.686
rhoCH[1]	1.938	0.3027	1.2703	2.413
rhoCH[2]	1.944	0.2992	1.3033	2.409
rhoCH[3]	1.955	0.2917	1.3271	2.411
rhoCH[4]	1.965	0.2847	1.3445	2.414
rhoCH[5]	1.978	0.2752	1.4042	2.416
rhoCH[6]	1.989	0.2672	1.4379	2.414
rhoCH[7]	2.003	0.2602	1.4550	2.421
rhoCH[8]	2.018	0.2548	1.4782	2.423
rhoCH[9]	2.035	0.2462	1.5084	2.429
rhoCH[10]	2.051	0.2388	1.5454	2.438
rhoCH[11]	2.065	0.2257	1.5823	2.429
rhoCH[12]	2.080	0.2182	1.6132	2.436
rhoCH[13]	2.094	0.2069	1.6351	2.430
rhoCH[14]	2.107	0.1996	1.6690	2.439
rhoCH[15]	2.121	0.1873	1.7156	2.430
rhoCH[16]	2.131	0.1808	1.7426	2.437
rhoCH[17]	2.144	0.1688	1.7918	2.433
rhoCH[18]	2.163	0.1567	1.8315	2.432
rhoCH[19]	2.187	0.1485	1.8687	2.438
rhoCH[20]	2.204	0.1405	1.9044	2.466
rhoCH[21]	2.222	0.1387	1.9473	2.486
rhoCH[22]	2.227	0.1349	1.9483	2.489
rhoCH[23]	2.246	0.1334	1.9813	2.507
rhoCH[24]	2.256	0.1303	1.9878	2.517
rhoCH[25]	2.260	0.1270	1.9990	2.514
rhoCH[26]	2.270	0.1235	2.0228	2.525
rhoCH[27]	2.277	0.1174	2.0395	2.507

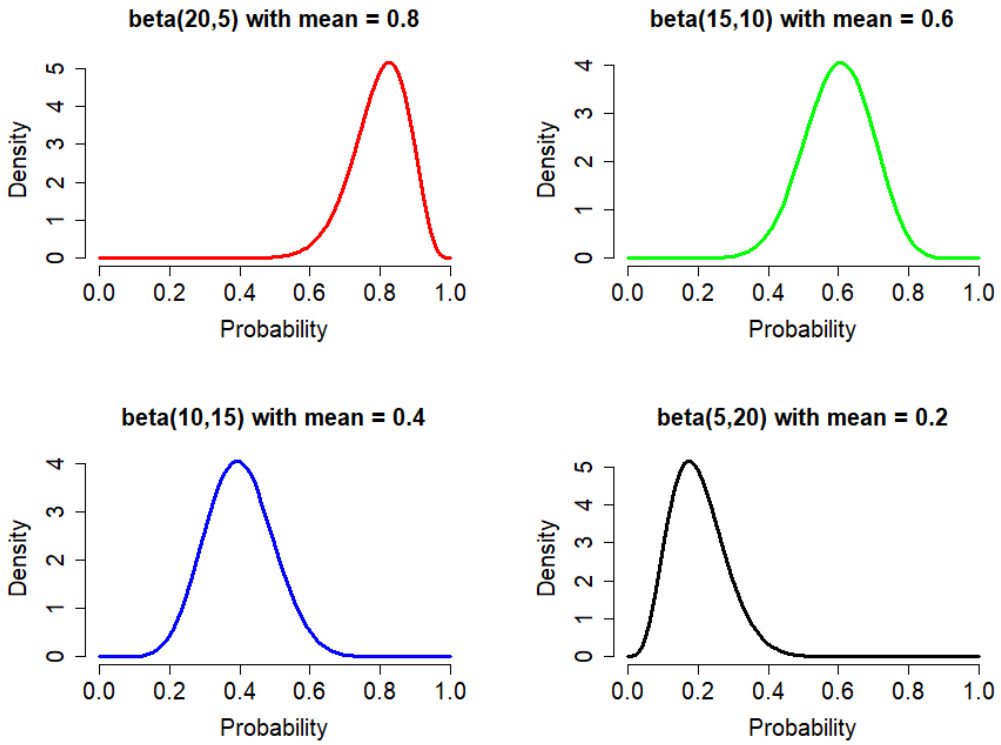
rhoCH[28]	2.290	0.1158	2.0671	2.526
rhoCH[29]	2.302	0.1136	2.0750	2.544
rhoCH[30]	2.321	0.1113	2.1175	2.564
rhoCH[31]	2.346	0.1131	2.1578	2.600
rhoCH[32]	2.354	0.1145	2.1701	2.614
rhoCH[33]	2.347	0.1085	2.1591	2.593
rhoCH[34]	2.348	0.1077	2.1684	2.577
rhoCH[35]	2.331	0.1015	2.1399	2.549
rhoCH[36]	2.311	0.1012	2.1111	2.514
rhoCH[37]	2.315	0.1030	2.1146	2.529
rhoCH[38]	2.312	0.1071	2.1054	2.530
rhoCH[39]	2.324	0.1048	2.1234	2.547
rhoCH[40]	2.352	0.1116	2.1607	2.604
rhoCH[41]	2.350	0.1068	2.1644	2.594
rhoCH[42]	2.327	0.1008	2.1390	2.535
rhoCH[43]	2.314	0.1009	2.1027	2.514
rhoCH[44]	2.339	0.1021	2.1436	2.562
rhoCH[45]	2.353	0.1045	2.1675	2.578
rhoCH[46]	2.366	0.1113	2.1743	2.611
rhoCH[47]	2.371	0.1151	2.1679	2.629
rhoCH[48]	2.368	0.1206	2.1731	2.643
rhoCH[49]	2.351	0.1155	2.1564	2.628
rhoCH[50]	2.316	0.1116	2.1127	2.570
rhoCH[51]	2.288	0.1091	2.0753	2.522
rhoCH[52]	2.263	0.1100	2.0362	2.490
rhoCH[53]	2.227	0.1186	1.9762	2.447
rhoCH[54]	2.191	0.1288	1.9061	2.408
rhoCH[55]	2.179	0.1320	1.8908	2.415
rhoCH[56]	2.175	0.1305	1.9034	2.412
rhoCH[57]	2.162	0.1348	1.8822	2.399
rhoCH[58]	2.150	0.1398	1.8616	2.401
rhoCH[59]	2.151	0.1454	1.8435	2.403
rhoCH[60]	2.148	0.1568	1.8090	2.410
rhoF[1]	1.313	0.1473	1.0412	1.625
rhoF[2]	1.338	0.1378	1.0760	1.633
rhoF[3]	1.367	0.1293	1.1324	1.644
rhoF[4]	1.393	0.1264	1.1533	1.650
rhoF[5]	1.412	0.1298	1.1683	1.672
rhoF[6]	1.413	0.1321	1.1611	1.673
rhoF[7]	1.424	0.1330	1.1704	1.689
rhoF[8]	1.457	0.1313	1.1934	1.709
rhoF[9]	1.504	0.1277	1.2583	1.755
rhoF[10]	1.558	0.1245	1.3149	1.810
rhoF[11]	1.615	0.1247	1.3905	1.871
rhoF[12]	1.655	0.1204	1.4283	1.904
rhoF[13]	1.686	0.1177	1.4549	1.930
rhoF[14]	1.711	0.1128	1.4913	1.936
rhoF[15]	1.747	0.1100	1.5339	1.974
rhoF[16]	1.801	0.1088	1.5963	2.015
rhoF[17]	1.843	0.1089	1.6448	2.065
rhoF[18]	1.870	0.1087	1.6658	2.100
rhoF[19]	1.863	0.1024	1.6633	2.075
rhoF[20]	1.841	0.1023	1.6323	2.038
rhoF[21]	1.875	0.1027	1.6737	2.069
rhoF[22]	1.924	0.1015	1.7271	2.124
rhoF[23]	1.994	0.0977	1.8088	2.194

rhoF[24]	2.038	0.0988	1.8574	2.230
rhoF[25]	2.090	0.0980	1.9084	2.291
rhoF[26]	2.202	0.1038	2.0165	2.411
rhoF[27]	2.292	0.1056	2.1026	2.515
rhoF[28]	2.326	0.1038	2.1372	2.545
rhoF[29]	2.268	0.0947	2.0808	2.462
rhoF[30]	2.288	0.0990	2.1087	2.487
rhoF[31]	2.247	0.0994	2.0483	2.446
rhoF[32]	2.270	0.1008	2.0704	2.480
rhoF[33]	2.344	0.1033	2.1426	2.553
rhoF[34]	2.372	0.1015	2.1852	2.581
rhoF[35]	2.362	0.1045	2.1675	2.574
rhoF[36]	2.310	0.1055	2.1029	2.515
rhoF[37]	2.328	0.0999	2.1394	2.533
rhoF[38]	2.317	0.1049	2.1114	2.522
rhoF[39]	2.334	0.1012	2.1500	2.544
rhoF[40]	2.336	0.1079	2.1368	2.557
rhoF[41]	2.285	0.1035	2.0987	2.503
rhoF[42]	2.217	0.0987	2.0114	2.410
rhoF[43]	2.166	0.0949	1.9836	2.353
rhoF[44]	2.162	0.0928	1.9810	2.347
rhoF[45]	2.164	0.0915	1.9884	2.343
rhoF[46]	2.171	0.0910	2.0032	2.362
rhoF[47]	2.156	0.0904	1.9866	2.350
rhoF[48]	2.110	0.0881	1.9444	2.290
rhoF[49]	1.987	0.0835	1.8282	2.151
rhoF[50]	1.895	0.0918	1.7092	2.065
rhoF[51]	1.919	0.0832	1.7479	2.078
rhoF[52]	1.959	0.0850	1.7958	2.128
rhoF[53]	1.947	0.0894	1.7755	2.128
rhoF[54]	1.962	0.0870	1.7911	2.139
rhoF[55]	1.973	0.0880	1.8015	2.146
rhoF[56]	2.064	0.0938	1.8872	2.252
rhoF[57]	2.078	0.0870	1.9163	2.263
rhoF[58]	2.056	0.0837	1.8998	2.221
rhoF[59]	2.037	0.0879	1.8749	2.211
rhoF[60]	1.957	0.1016	1.7664	2.156
r[1]	0.129	0.0326	0.0743	0.201
r[2]	0.127	0.0313	0.0743	0.195
r[3]	0.125	0.0300	0.0741	0.190
r[4]	0.123	0.0287	0.0738	0.185
r[5]	0.121	0.0275	0.0736	0.180
r[6]	0.119	0.0263	0.0733	0.176
r[7]	0.117	0.0251	0.0730	0.171
r[8]	0.115	0.0240	0.0727	0.167
r[9]	0.113	0.0229	0.0725	0.163
r[10]	0.111	0.0218	0.0724	0.157
r[11]	0.109	0.0208	0.0723	0.154
r[12]	0.107	0.0198	0.0722	0.150
r[13]	0.105	0.0188	0.0721	0.146
r[14]	0.104	0.0178	0.0717	0.141
r[15]	0.102	0.0169	0.0715	0.137
r[16]	0.100	0.0160	0.0714	0.134
r[17]	0.099	0.0151	0.0713	0.130
r[18]	0.097	0.0142	0.0712	0.126
r[19]	0.095	0.0134	0.0707	0.123

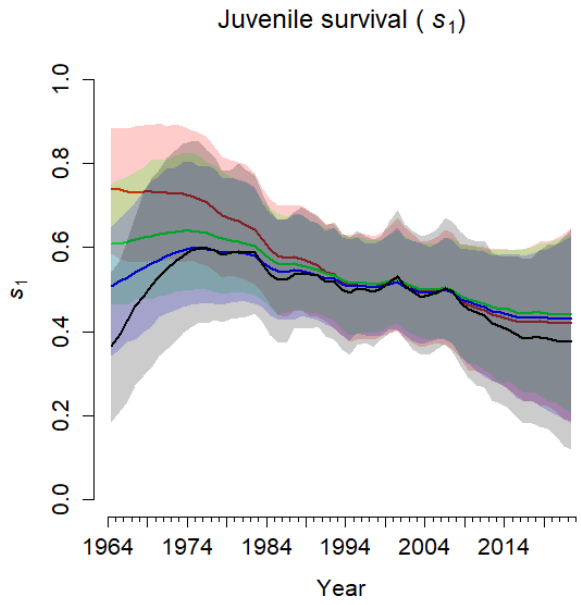
r[20]	0.094	0.0127	0.0705	0.120
r[21]	0.092	0.0119	0.0702	0.117
r[22]	0.091	0.0112	0.0699	0.114
r[23]	0.089	0.0105	0.0696	0.111
r[24]	0.088	0.0098	0.0692	0.108
r[25]	0.086	0.0092	0.0689	0.105
r[26]	0.085	0.0087	0.0686	0.102
r[27]	0.084	0.0081	0.0682	0.100
r[28]	0.082	0.0076	0.0679	0.098
r[29]	0.081	0.0072	0.0673	0.095
r[30]	0.080	0.0068	0.0667	0.093
r[31]	0.078	0.0064	0.0659	0.091
r[32]	0.077	0.0061	0.0653	0.089
r[33]	0.076	0.0059	0.0645	0.087
r[34]	0.074	0.0057	0.0638	0.086
r[35]	0.073	0.0056	0.0631	0.084
r[36]	0.072	0.0055	0.0619	0.083
r[37]	0.071	0.0055	0.0609	0.082
r[38]	0.070	0.0055	0.0597	0.081
r[39]	0.069	0.0056	0.0584	0.080
r[40]	0.068	0.0057	0.0572	0.079
r[41]	0.066	0.0059	0.0559	0.078
r[42]	0.065	0.0061	0.0543	0.078
r[43]	0.064	0.0063	0.0526	0.077
r[44]	0.063	0.0065	0.0511	0.077
r[45]	0.062	0.0067	0.0497	0.076
r[46]	0.061	0.0070	0.0485	0.076
r[47]	0.060	0.0072	0.0472	0.076
r[48]	0.059	0.0075	0.0458	0.076
r[49]	0.059	0.0077	0.0445	0.075
r[50]	0.058	0.0080	0.0433	0.075
r[51]	0.057	0.0082	0.0419	0.075
r[52]	0.056	0.0085	0.0408	0.075
r[53]	0.055	0.0087	0.0395	0.074
r[54]	0.054	0.0090	0.0384	0.074
r[55]	0.053	0.0092	0.0372	0.074
r[56]	0.052	0.0095	0.0359	0.074
r[57]	0.052	0.0097	0.0349	0.074
r[58]	0.051	0.0099	0.0338	0.073
r[59]	0.050	0.0101	0.0327	0.073

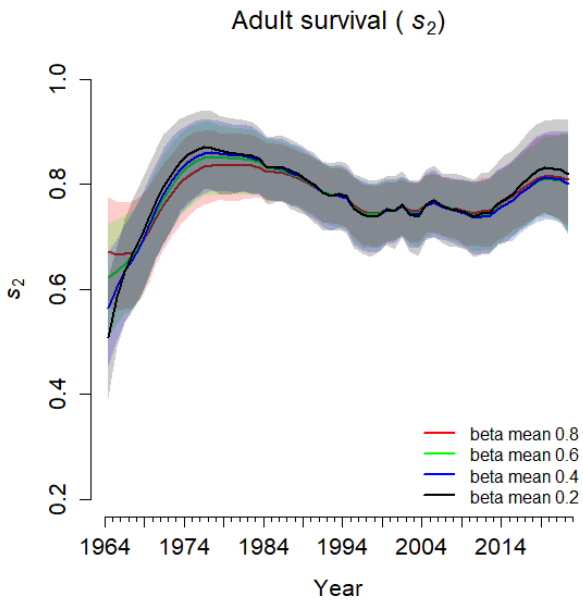
Appendix S8: Prior sensitivity analysis of the main result of our study: the increase in adult survival during the early years of the study, i.e., during the pesticide crash.

We re-fitted the main random-walk model four times, with the following four different informative priors on the survival probability during the initial survival interval, 1964–1965.

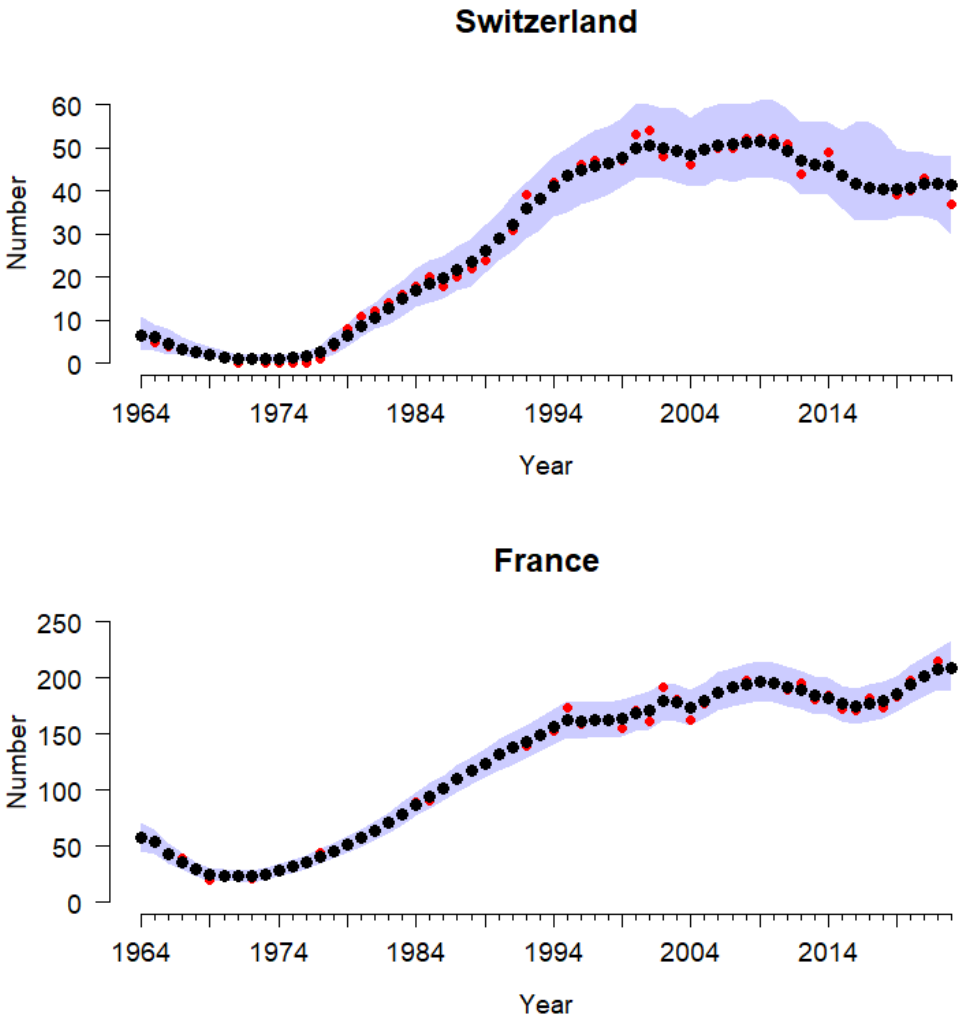


This resulted in the following estimated trajectories for juvenile and adult survival (posterior means and 95% CRIs are shown), and where the color coding matches that in the above figure showing the priors adopted in each.

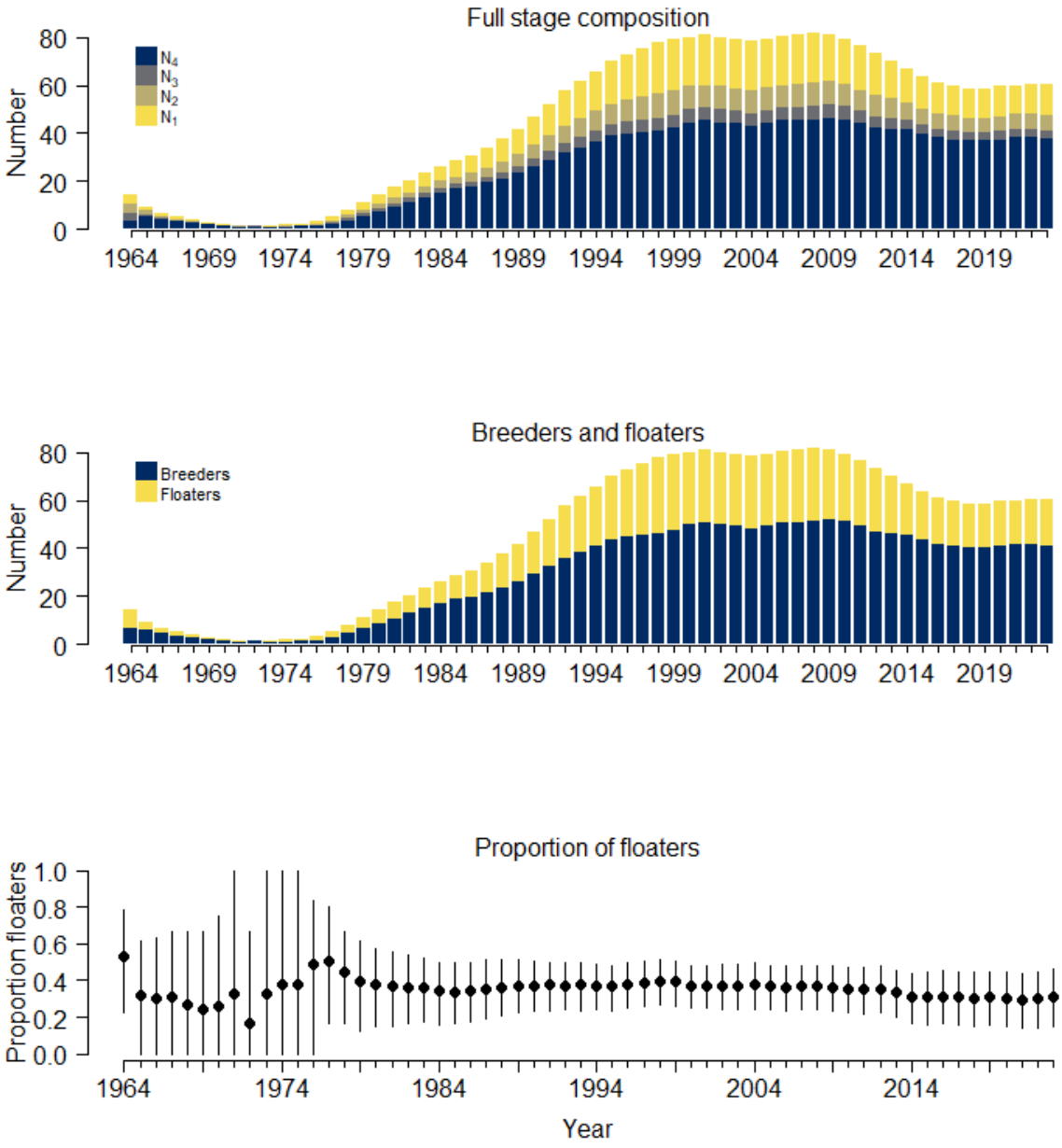

Juvenile survival (s_1)
s_1
0.0
0.2
0.4
0.6
0.8
1.0
1964
1974
1984
1994
2004
2014
Year


Adult survival (s_2)
s_2
0.2
0.4
0.6
0.8
1.0
1964
1974
1984
1994
2004
2014
Year
beta mean 0.8
beta mean 0.6
beta mean 0.4
beta mean 0.2

Appendix S9: Estimated trajectories of the number of breeding pairs in the Swiss and the French long-term study (posterior means with 95% CRIs). Red symbols show the observed counts of territorial pairs. Note different scaling of the y-axis.



Appendix S10: Stage distributions of the population, and proportion of floaters, in the Swiss study area under the random-walk model fit to the data from both study areas.



Appendix S11: Stage distributions of the population, and proportion of floaters, in the French study area under the random-walk model fit to the data from both study areas.

